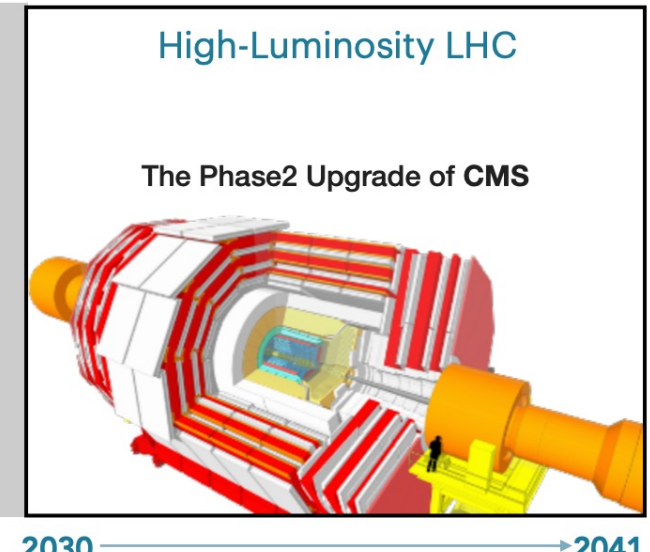
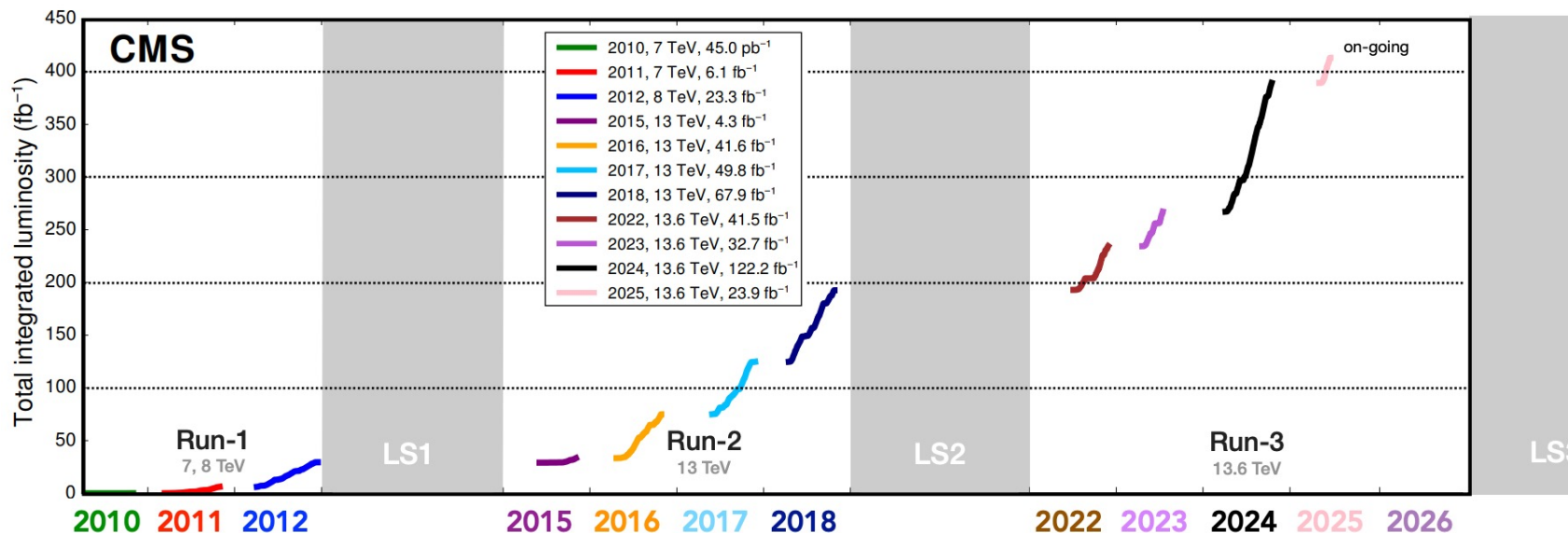




CMS Heavy Meson FCNC results



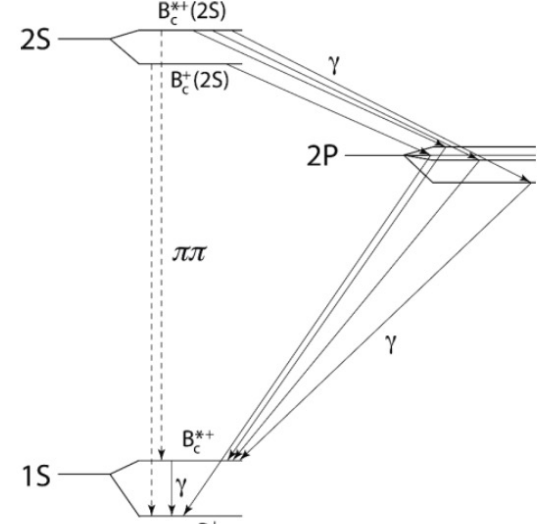
Dayong Wang
Peking University



CMS Heavy spectroscopy: conventional and exotic

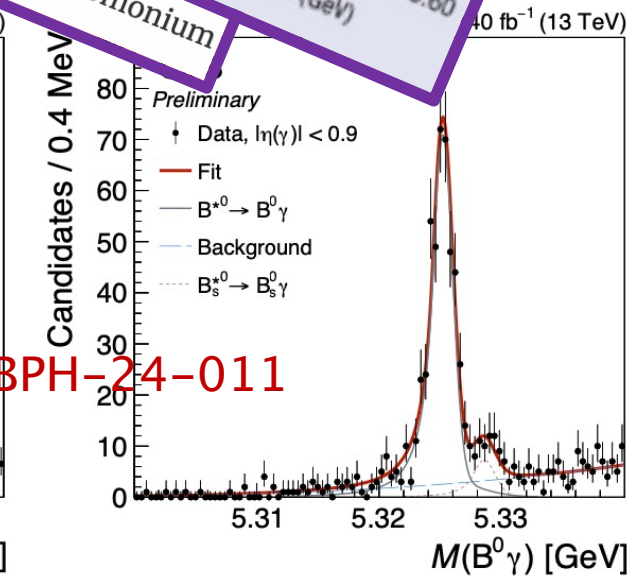
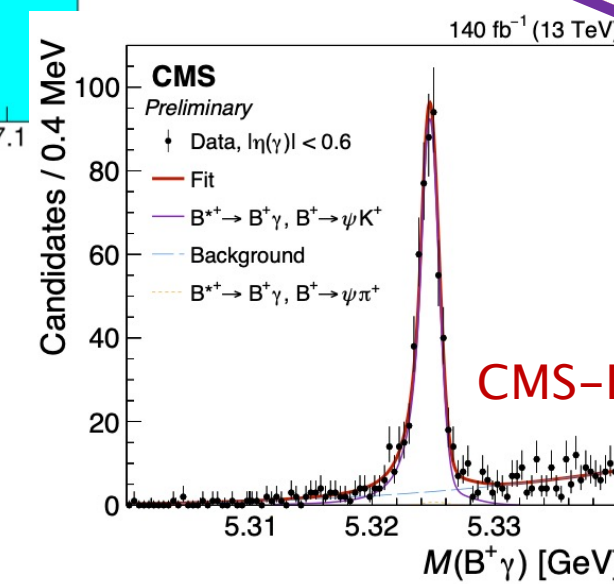
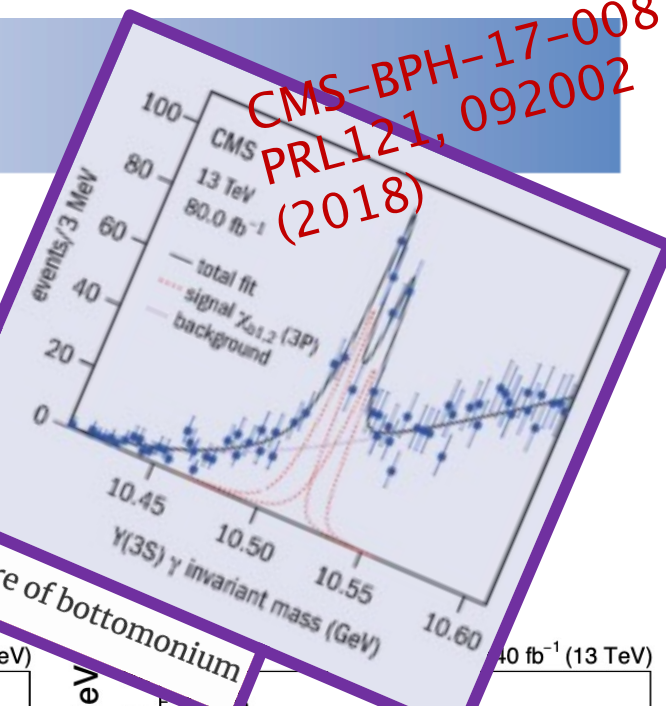
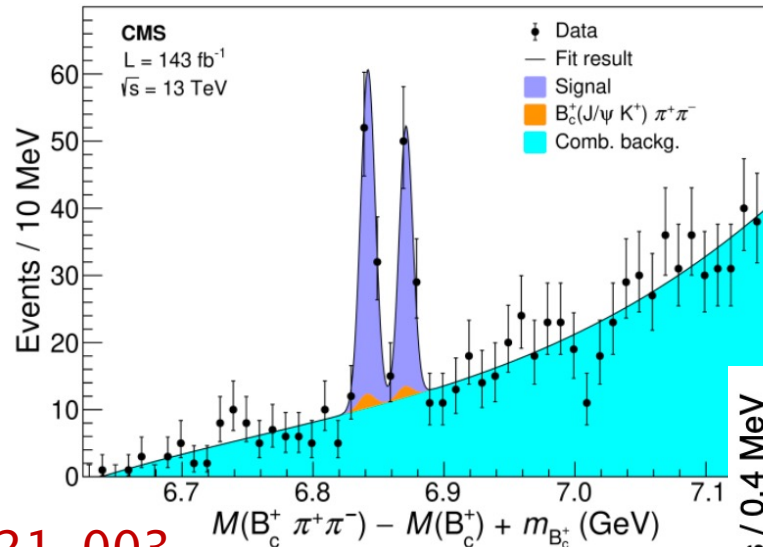
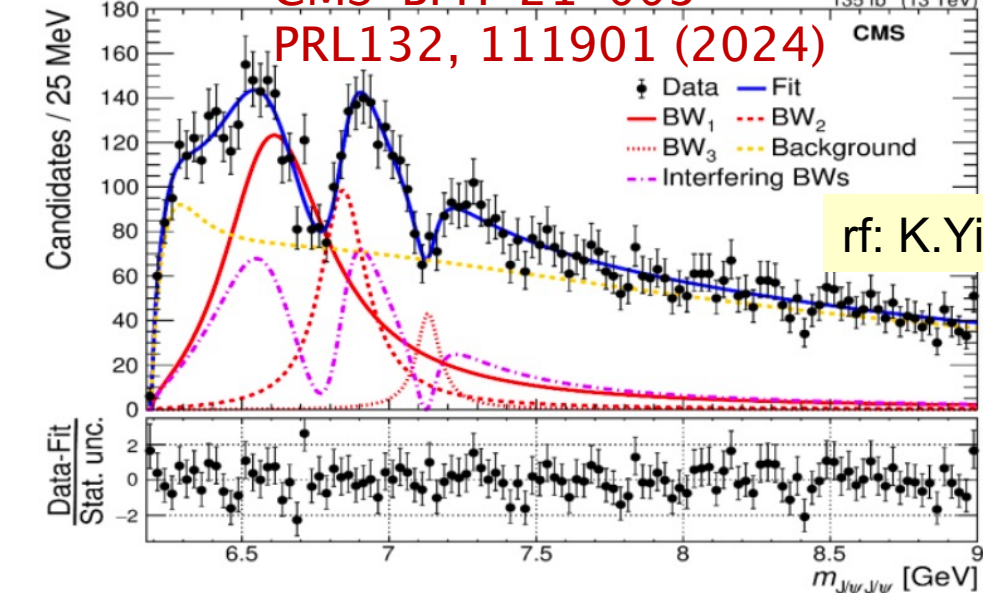
CMS-BPH-18-007

PRL122, 132001 (2019)



CMS-BPH-21-003

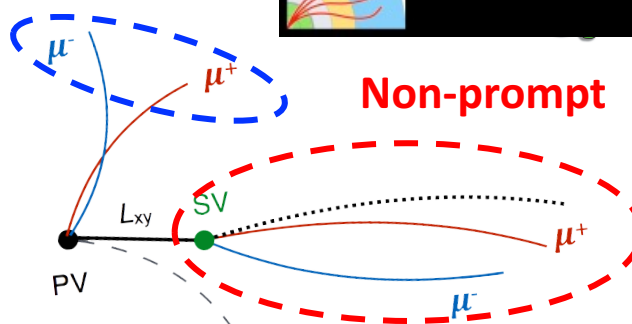
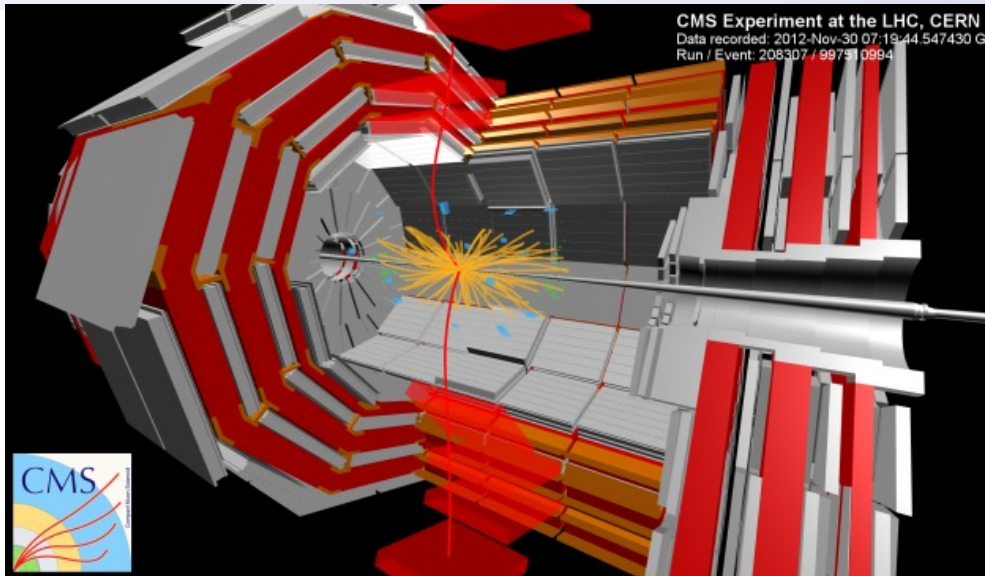
PRL132, 111901 (2024)



$$\begin{aligned}\Delta m(B^{*+}) &\equiv m(B^{*+}) - m(B^+) & 45.277 \pm 0.039 \pm 0.021 \text{ MeV} \\ \Delta m(B^{*0}) &\equiv m(B^{*0}) - m(B^0) & 45.471 \pm 0.056 \pm 0.024 \text{ MeV} \\ \Delta m(B_s^{*0}) &\equiv m(B_s^{*0}) - m(B_s^0) & 49.407 \pm 0.132 \pm 0.034 \text{ MeV}\end{aligned}$$



Why CMS is marvelous for heavy hadron studies



Non-prompt

- Flexible trigger and data-taking schemes

Physics Reports 1115 (2025) 678–772

Contents lists available at ScienceDirect



Physics Reports

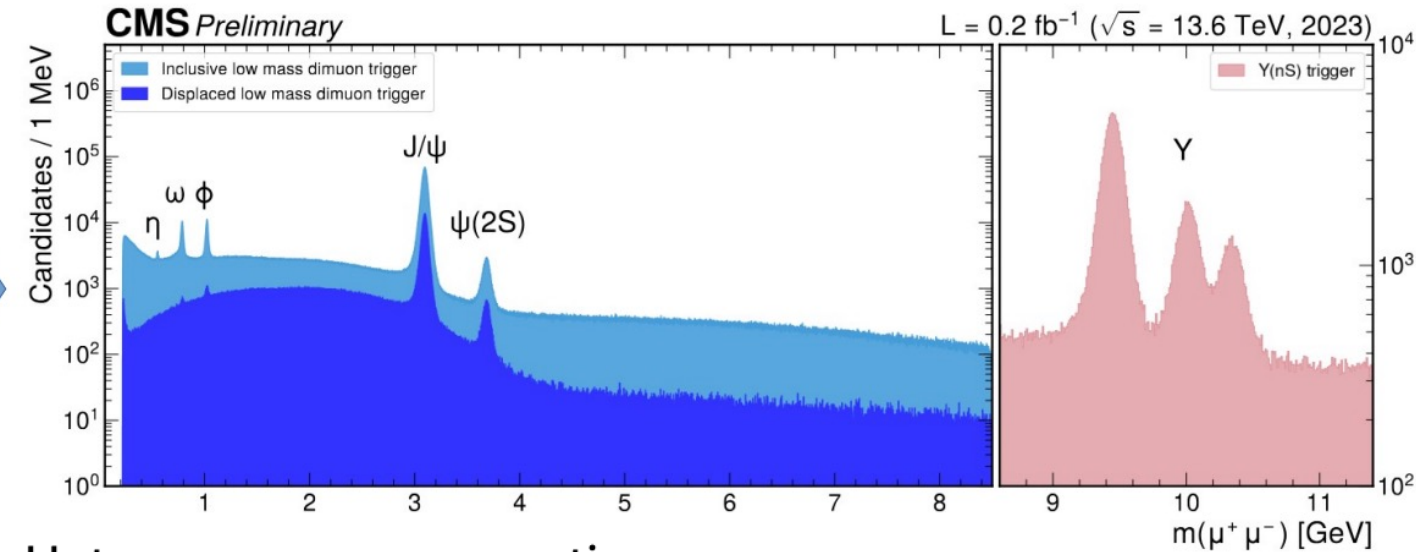
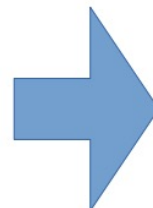
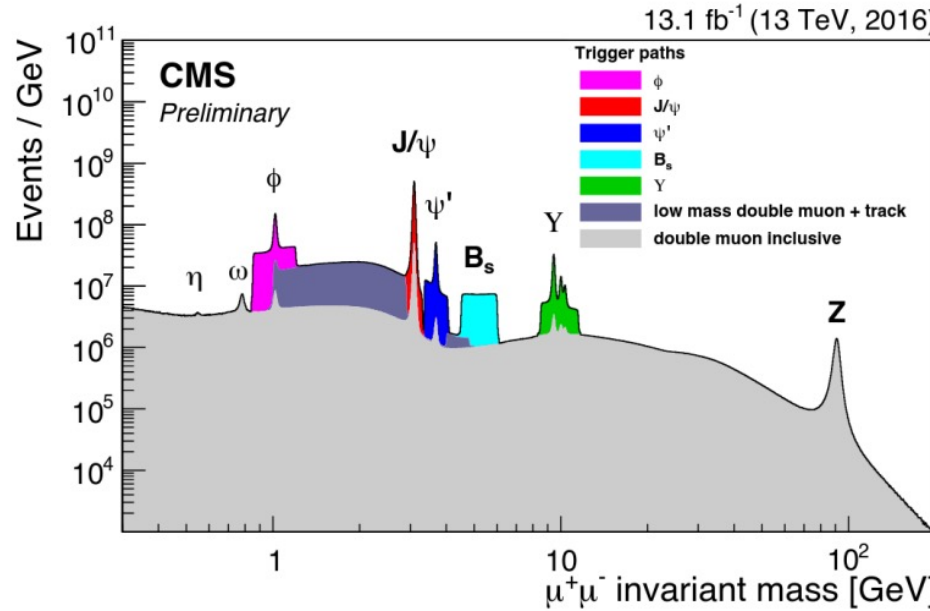
Physics Reports 1115 (2025) 678–77

journal homepage: www.elsevier.com/locate/physrep

Enriching the physics program of the CMS experiment via data scouting and data parking

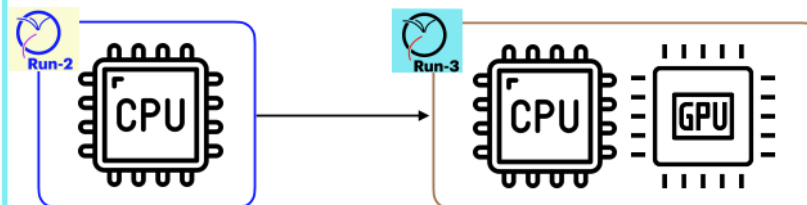
The CMS Collaboration

Evolution of BPH triggers



Heterogeneous computing

Successful R&D effort to run the High-Level Trigger reconstruction on heterogeneous hardware in production since the start of Run-3



Faster and more power-efficient HLT reconstruction

+50% event processing throughput
+15-25% performance per kW

Portable heterogeneous software (Alpaka) deployed
same code base can run seamlessly on CPUs and GPUs

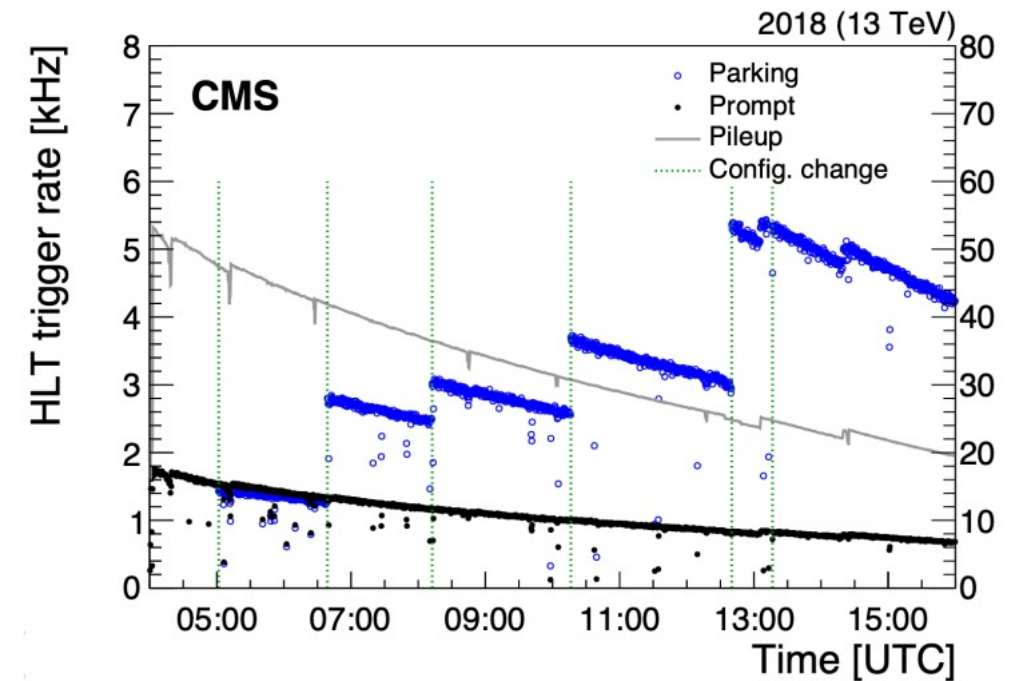
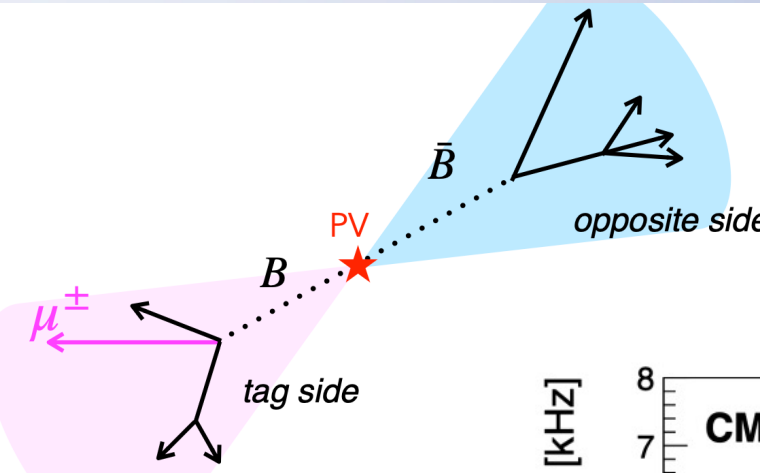
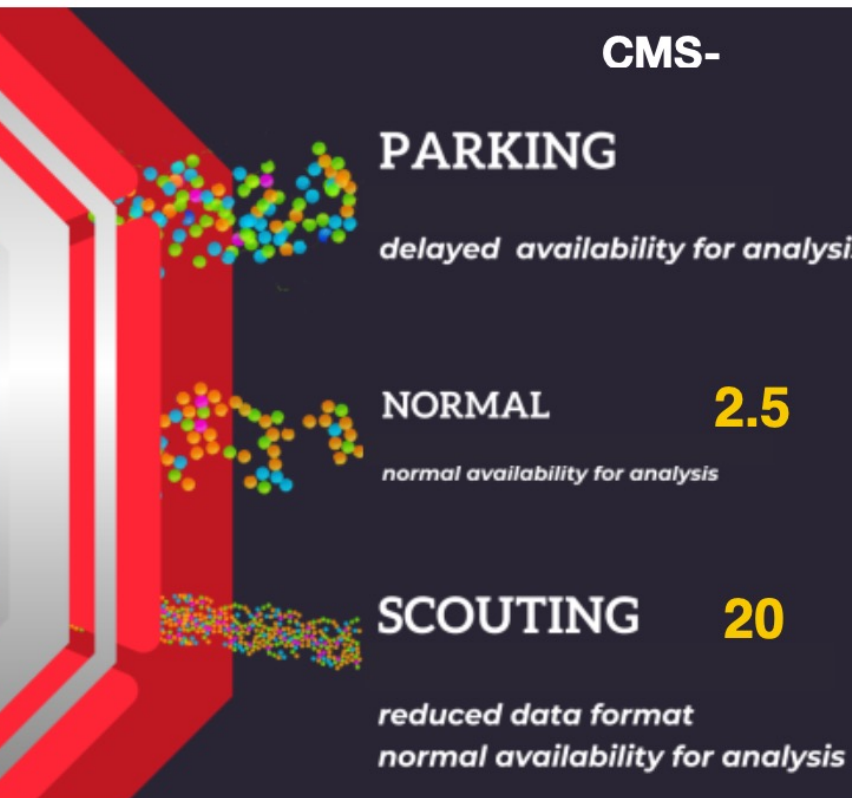


w/ Eric and Wendy Schmidt Fund for Strategic Innovation

- Many heavy-hadron analyses in CMS rely on dimuon triggers
- we moved from a set of triggers dedicated to specific dimuon mass regions or topologies, to an inclusive dimuon trigger with loose requirements on the momenta



Data Parking and scouting



Greatly increase the event rate we can take and used in analysis

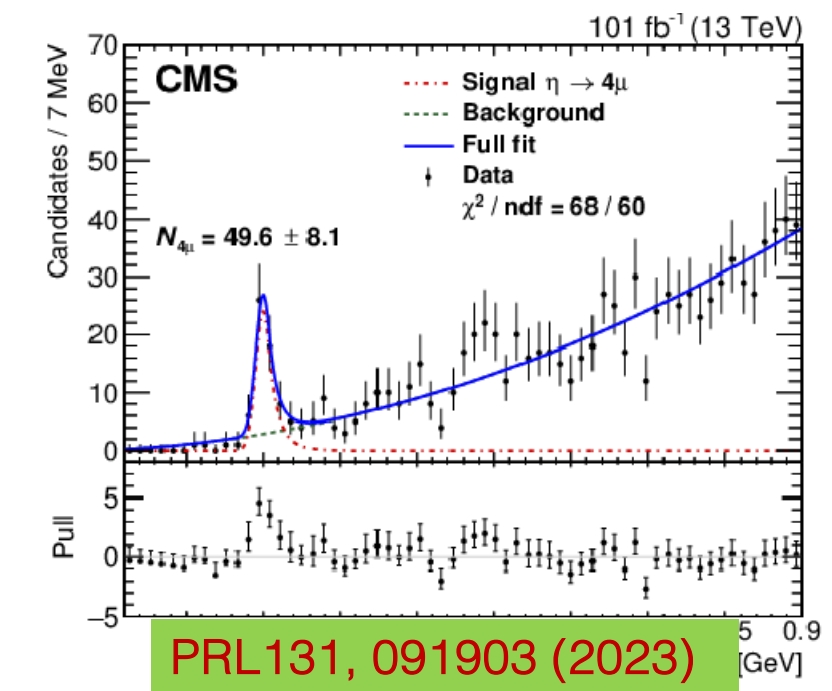
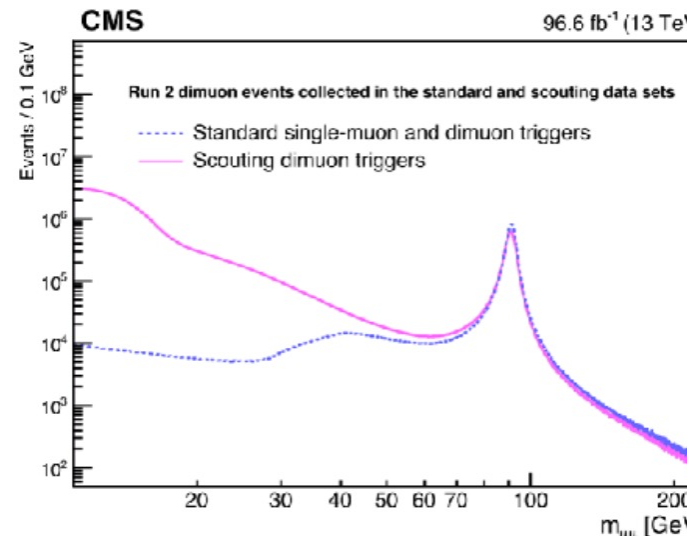
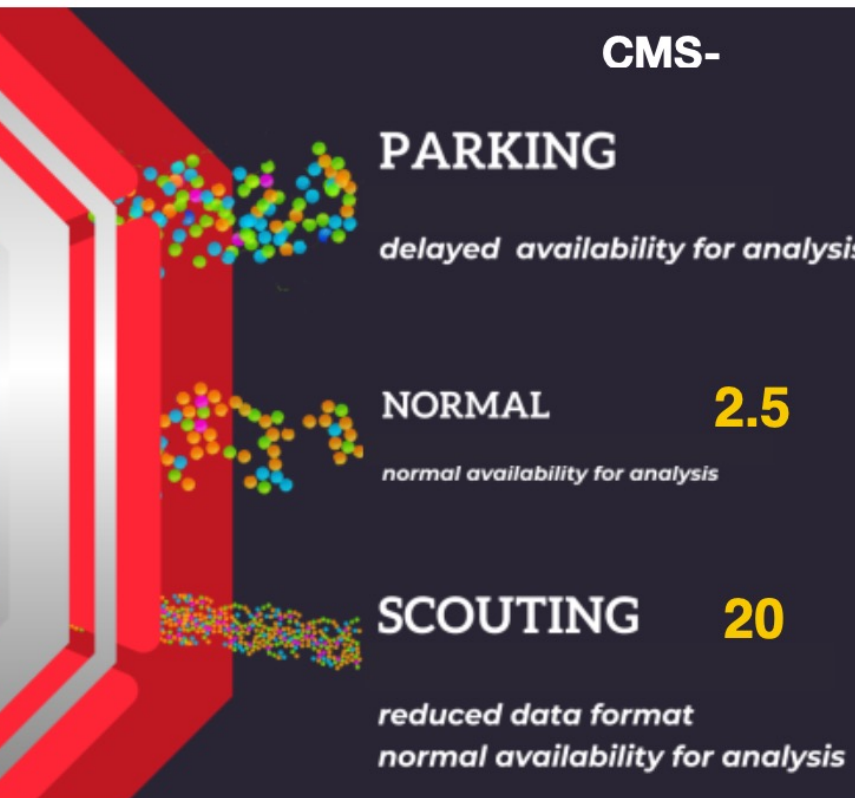
Run2018 Displaced Single Muon Dataset
12B events useful events were collected



Data Parking and scouting



- Selected L1 Triggers feed into stream with higher HLT rate and reduced content events for specific signatures
- Two streams: jets and muons

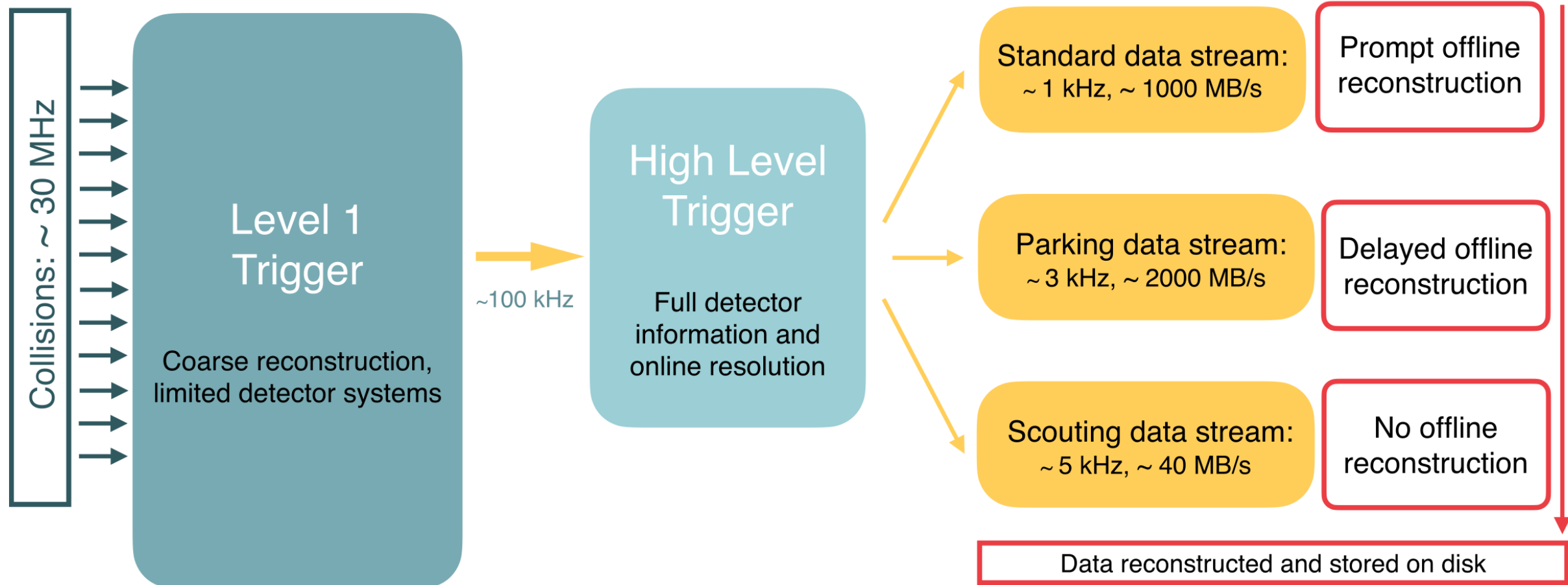


opening up otherwise inaccessible low-mass phase space

$$\mathcal{B}(\eta \rightarrow \mu^+ \mu^- \mu^+ \mu^-) = (5.0 \pm 0.8 \text{ (stat)} \pm 0.7 \text{ (syst)} \pm 0.7 (\mathcal{B}_{2\mu})) \times 10^{-9}$$



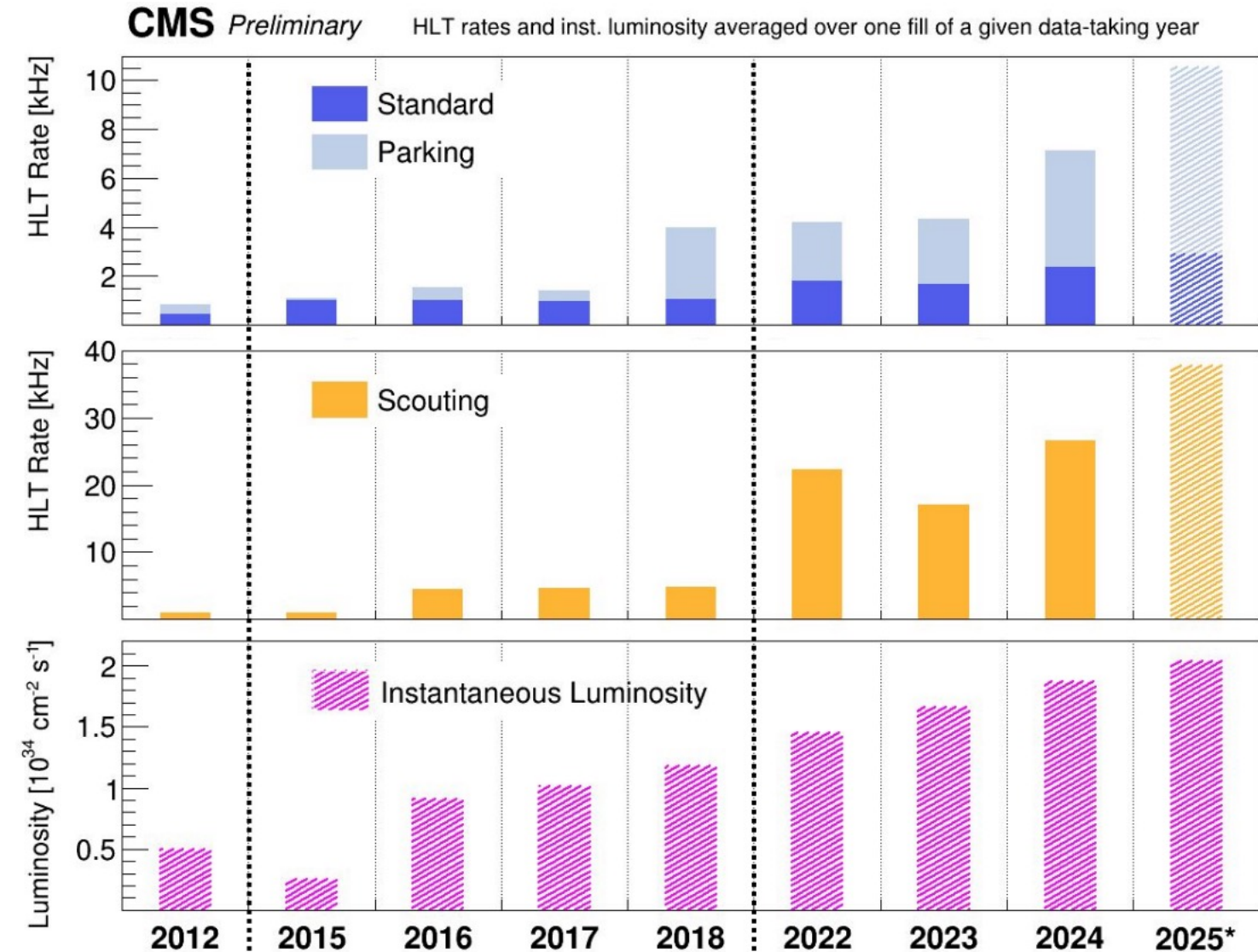
CMS data taking scheme(RunII)





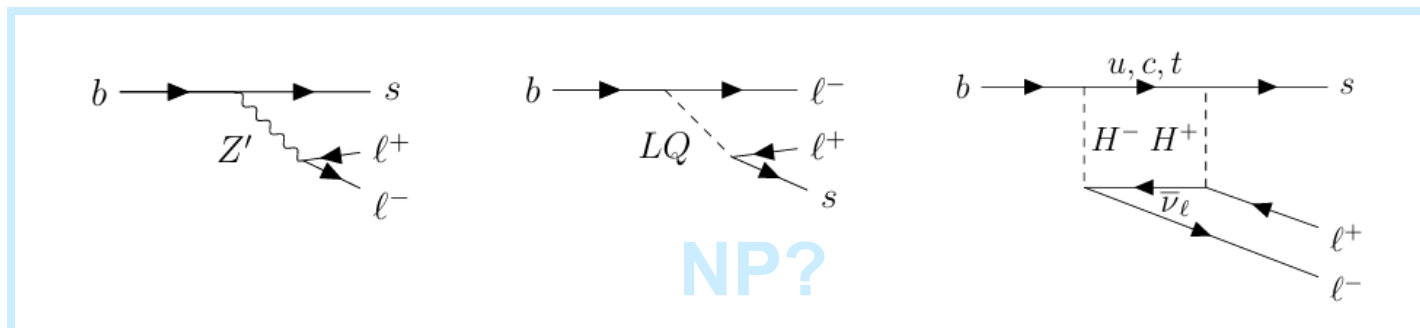
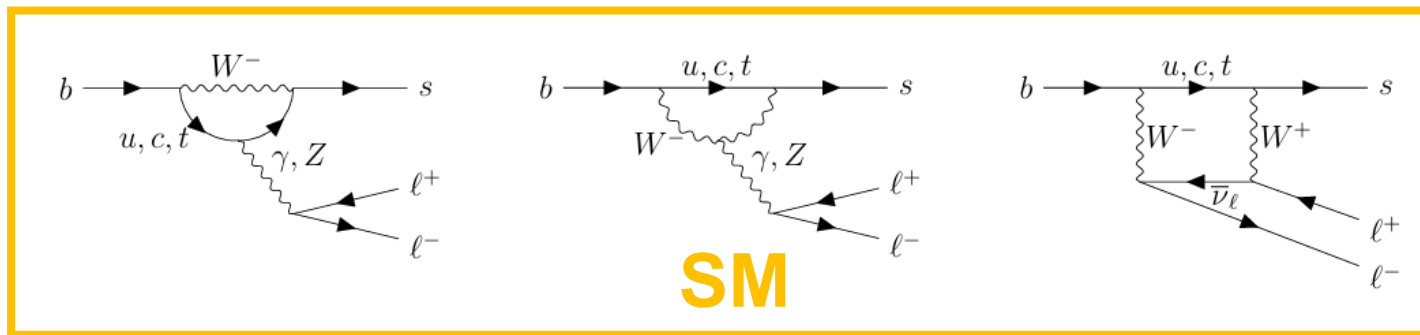
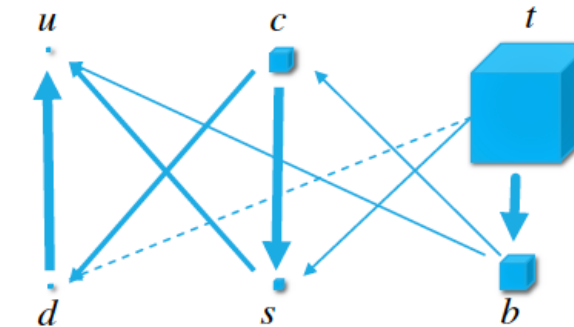
CMS coverage far beyond design values

- ◆ **Parking is now integral to the core physics program (Higgs, searches, etc.), and opens large phase space for flavour physics**
- ◆ **HLT scouting runs at ~30 kHz (1/3 of accepted L1T events)**
 - Using HLT objects for physics analyses in an even wider phase space

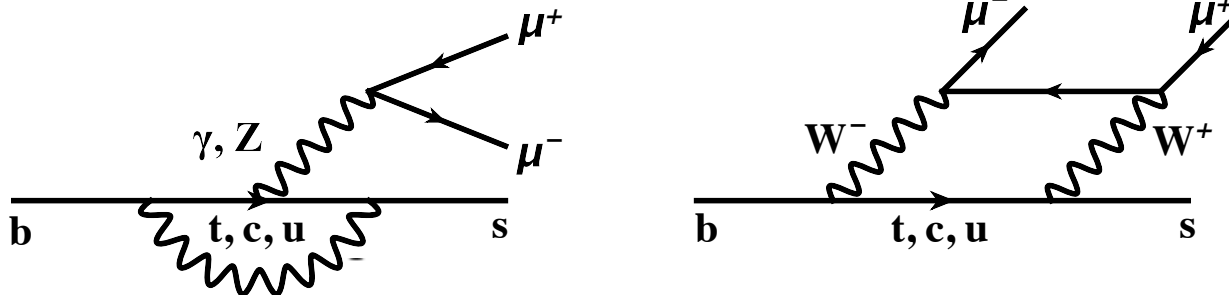


味改变的中性流过程

- Flavour-changing-neutral-current (FCNC) transition: transitions between quarks of the same electric charge
- SM: forbidden at tree level, need more complex diagrams to achieve
- Enhanced in many BSM theories: new particles can contribute at the loop or tree level
- NP can modify angular parameters, decay rates ...



FCNC processes $b \rightarrow s\mu^+\mu^-$: golden indirect probes of NP



$$\mathcal{H}_{\text{eff}} = -\frac{4G_F}{\sqrt{2}} V_{tb} V_{tq}^* \sum_i \underbrace{\mathcal{C}_i \mathcal{O}_i}_{\text{Left handed}} + \underbrace{\mathcal{C}'_i \mathcal{O}'_i}_{\text{Right handed, } \frac{m_s}{m_b} \text{ suppressed}} + \sum \frac{c}{\Lambda_{\text{NP}}^2} \mathcal{O}_{\text{NP}}$$

$i = 1, 2$	Tree
$i = 3 - 6, 8$	Gluon penguin
$i = 7$	Photon penguin
$i = 9, 10$	EW penguin
$i = S, P$	(Pseudo)scalar penguin

Effective theory: Different processes are sensitive to different operators

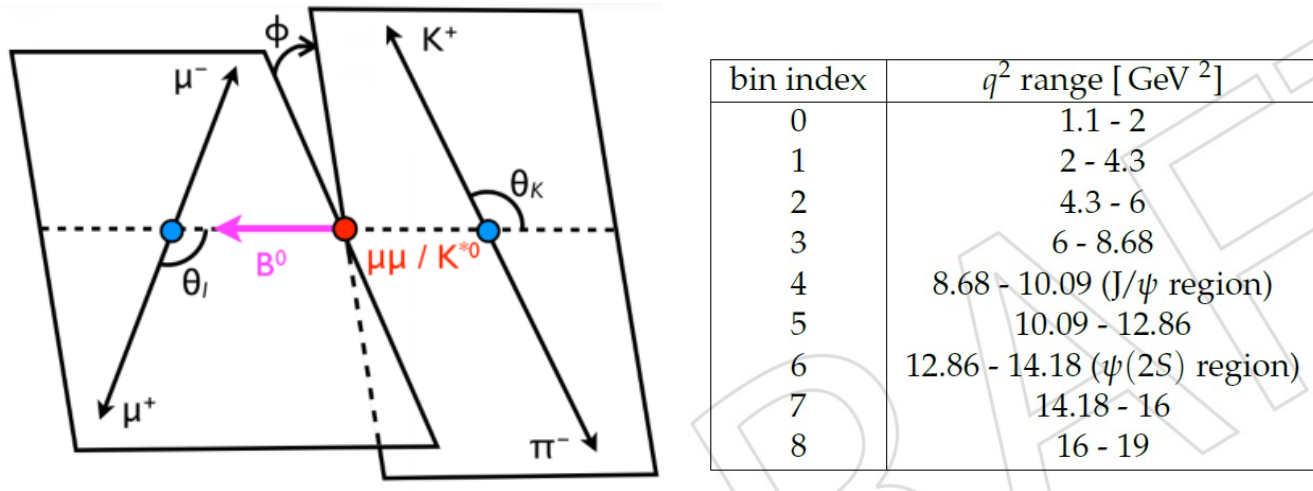
Operator \mathcal{O}_i	$B_{s,d} \rightarrow X_{s,d} \mu^+ \mu^-$	$B_{s,d} \rightarrow \mu^+ \mu^-$	$B_{s,d} \rightarrow X_{s,d} \gamma$
$\mathcal{O}_7 \sim m_b (\bar{s}_L \sigma^{\mu\nu} b_R) F_{\mu\nu}$	✓		✓
$\mathcal{O}_9 \sim (\bar{s}_L \gamma^\mu b_L)(\bar{\ell} \gamma_\mu \ell)$	✓		
$\mathcal{O}_{10} \sim (\bar{s}_L \gamma^\mu b_L)(\bar{\ell} \gamma_5 \gamma_\mu \ell)$	✓	✓	
$\mathcal{O}_{S,P} \sim (\bar{s}b)_{S,P} (\bar{\ell}\ell)_{S,P}$	(✓)	✓	

clean exp signature;
robust theory calc;
high sensitivity

$B^0 \rightarrow K^{*0} \mu\mu$ 过程的角分析

Angular analysis

- measure the rate of a decay process as a function of the angles of the final decay products
- Compared to measuring the branching fractions: give access to large range of observables with reduced theory uncertainties
- Can help deduce nature of new physics models



$B^0 \rightarrow K^{*0} \mu\mu$ can be fully described by the three angles $(\theta_l, \theta_k, \phi)$ and the dimuon invariant mass squared q^2

$$\cos \theta_l = (\hat{p}_{\mu^+}^{(\mu^+\mu^-)}) \cdot (-\hat{p}_{B^0}^{(\mu^+\mu^-)})$$

$$\cos \theta_K = (\hat{p}_{K^+}^{(K^{*0})}) \cdot (-\hat{p}_{B^0}^{(K^{*0})})$$

$$\cos \phi = (\hat{p}_{\mu^+}^{(B^0)} \times \hat{p}_{\mu^-}^{(B^0)}) \cdot (\hat{p}_{K^+}^{(B^0)} \times \hat{p}_{\pi^-}^{(B^0)})$$

$$\sin \phi = [(\hat{p}_{\mu^+}^{(B^0)} \times \hat{p}_{\mu^-}^{(B^0)}) \times (\hat{p}_{K^+}^{(B^0)} \times \hat{p}_{\pi^-}^{(B^0)})] \cdot \hat{p}_{K^{*0}}^{(B^0)}$$

Note: \hat{p}_x^y refers to the unit vector giving the direction of x in the rest frame



微分衰变率公式

Differential distribution:

$$\frac{1}{d\Gamma/dq^2} \frac{d^4\Gamma}{dq^2 d\cos\theta_l d\cos\theta_K d\phi} = \frac{9}{32\pi} \left[\frac{3}{4} F_T \sin^2 \theta_K + [F_L] \cos^2 \theta_K \right]$$

P'_i basis: form factor uncertainties
cancel at first order

$$P_1 = \frac{F_L}{2S_3}$$

$$P_2 = \frac{2}{3} \frac{A_{FB}}{1 - F_L}$$

$$P_3 = \frac{-S_9}{1 - F_L}$$

$$P'_{4,5,8} = \frac{S_{4,5,8}}{\sqrt{F_L(1 - F_L)}}$$

$$P'_6 = \frac{S_7}{\sqrt{F_L(1 - F_L)}}$$

$$\begin{aligned} & + (\frac{1}{4} F_T \sin^2 \theta_K - F_L \cos^2 \theta_K) \cos 2\theta_l \\ & + \frac{1}{2} P_1 F_T \sin^2 \theta_K \sin^2 \theta_l \cos 2\phi \\ & + \sqrt{F_T F_L} (\frac{1}{2} P'_4 \sin 2\theta_K \sin 2\theta_l \cos \phi + P'_5 \sin 2\theta_K \sin \theta_l \cos \phi) \\ & - \sqrt{F_T F_L} (P'_6 \sin 2\theta_K \sin \theta_l \sin \phi - \frac{1}{2} P'_8 \sin 2\theta_K \sin 2\theta_l \sin \phi) \\ & + 2P_2 F_T \sin^2 \theta_K \cos \theta_l - P_3 F_T \sin^2 \theta_K \sin^2 \theta_l \sin 2\phi)] \end{aligned}$$

$$\begin{aligned} & (1 - F_s) \Gamma_p + 2./3. (F_s \sin^2 \theta_l + A_s \sin^2 \theta_l \cos \theta_K \\ & + A_s^4 \sin \theta_K \sin 2\theta_l \cos \phi + A_s^5 \sin \theta_K \sin \theta_l \cos \phi \\ & + A_s^7 \sin \theta_K \sin \theta_l \sin \phi + A_s^8 \sin \theta_K \sin 2\theta_l \sin \phi) \end{aligned}$$

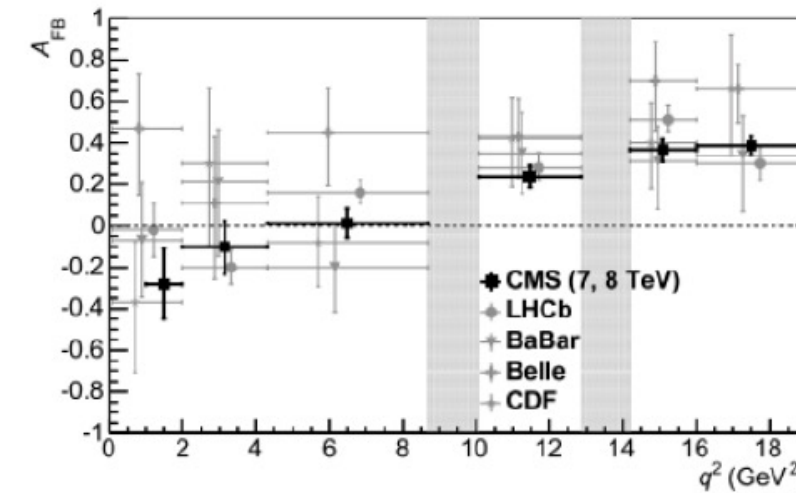
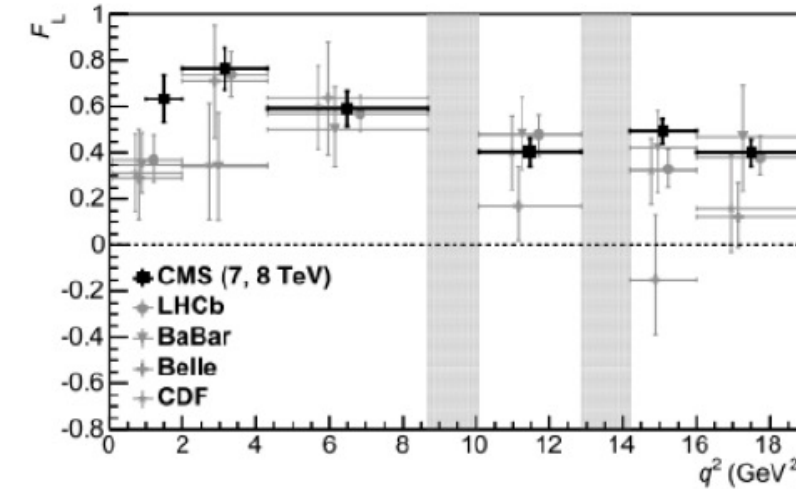
Additional terms account for contaminations
from **S-wave component and the interference** for the system of $B^0 \rightarrow K\pi\mu\mu$

- 8 angular parameters
- Sensitive to the Wilson coefficients
- $F_L, A_{FB}, S_i = f(C_7, C_9, C_{10})$
- $F_T = 1 - F_L$

实验测量的意义与历史: F_L and A_{FB}

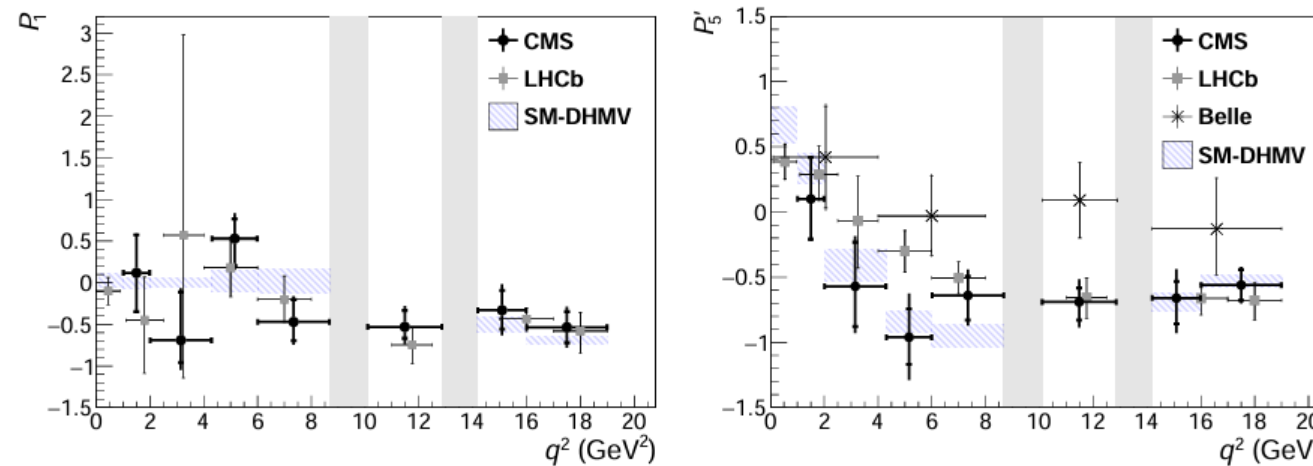
FCNC processes $b \rightarrow s l^+ l^-$ are not ultra rare, but provide an exceedingly rich set of observables to probe for NP effects, sensitive to non-SM helicity structures (and more).

- Long history of measurement at B-factories and hadron colliders
- Angular analysis with ATLAS, BaBar, Belle, CDF, CMS and LHCb
- No deviation from SM for F_L and A_{FB}



BaBar: PRD 86, 032012
 Belle: PRL 88, 021801
 PRL 103, 171801
 CDF: PRD 79, 031102
 PRL 108, 081807
 CMS: PLB 727 (2013) 77
 PLB 753 (2016) 424
 LHCb: JHEP 08 (2013) 131

- CMS performed partial angular analyses with Run-1 data, to measure F_L , A_{FB} and P_1 , P'_5 separately
 - Parameter space was reduced by integrating or folding the angular variable



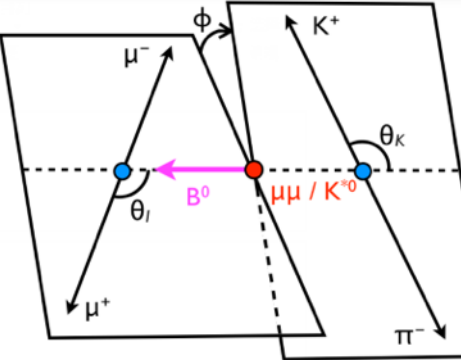
CMS: PLB 781 (2018) 517541
 LHCb: JHEP 02 (2016) 104
 Belle: PRL 118 (2017)
 SM: JHEP 01 (2013) 048, JHEP 05 (2013) 137

- P'_5 anomaly: $\sim 3\sigma$ discrepancy in some q^2 bin in LHCb results
- CMS Run2 collected 140 fb^{-1} of 13 TeV p-p data -> make it possible to perform a full angular analysis

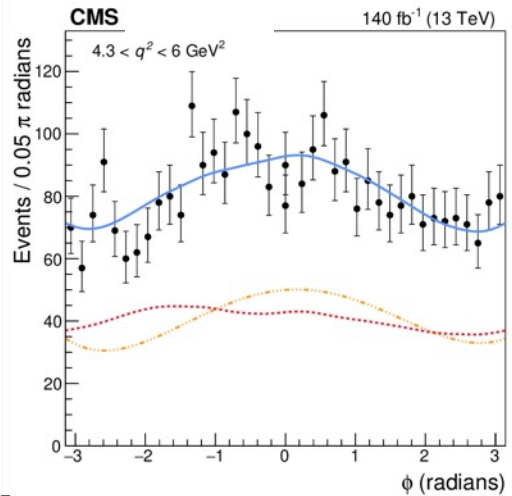
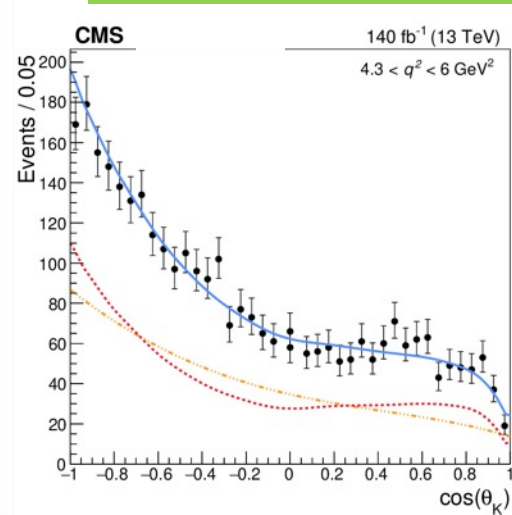
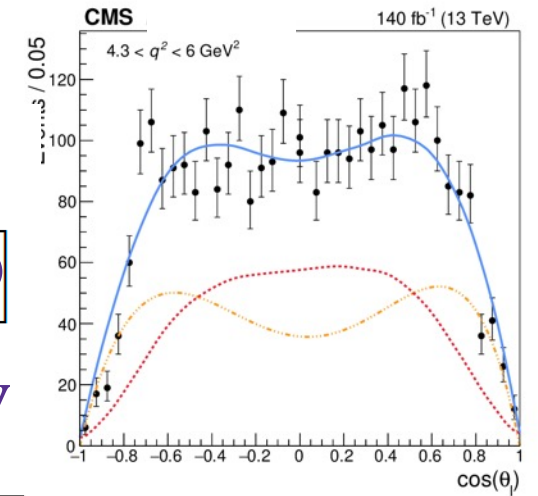
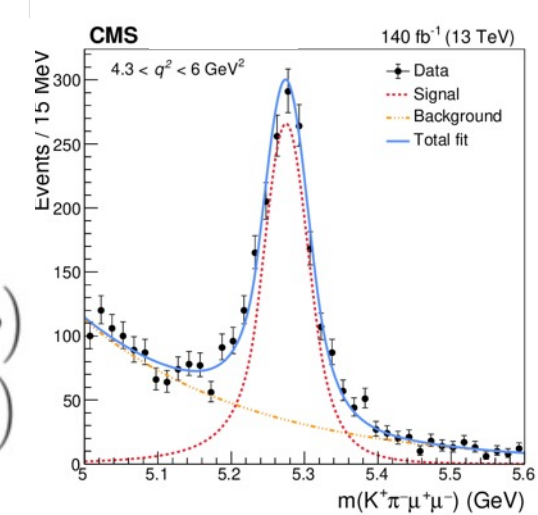
Run2: Full angular analysis of $B^0 \rightarrow K^{*0} \mu\mu$

CMS-BPH-21-002
PLB 864 (2025) 139406

$$\frac{1}{d\Gamma/dq^2} \frac{d^4\Gamma}{dq^2 d\cos\theta_l d\cos\theta_K d\phi} = \frac{9}{32\pi} \left[\frac{3}{4}(1-F_L) \sin^2\theta_K + \boxed{F_L} \cos^2\theta_K \right. \\ + \left(\frac{1}{4}(1-F_L) \sin^2\theta_K - F_L \cos^2\theta_K \right) \cos 2\theta_l \\ + \frac{1}{2} \boxed{P_1} (1-F_L) \sin^2\theta_K \sin^2\theta_l \cos 2\phi \\ + \sqrt{(1-F_L)F_L} \left(\frac{1}{2} \boxed{P'_4} \sin 2\theta_K \sin 2\theta_l \cos\phi + \boxed{P'_5} \sin 2\theta_K \sin\theta_l \cos\phi \right) \\ - \sqrt{(1-F_L)F_L} \left(\boxed{P'_6} \sin 2\theta_K \sin\theta_l \sin\phi - \frac{1}{2} \boxed{P'_8} \sin 2\theta_K \sin 2\theta_l \sin\phi \right) \\ \left. + 2 \boxed{P_2} (1-F_L) \sin^2\theta_K \cos\theta_l - \boxed{P_3} (1-F_L) \sin^2\theta_K \sin^2\theta_l \sin 2\phi \right],$$



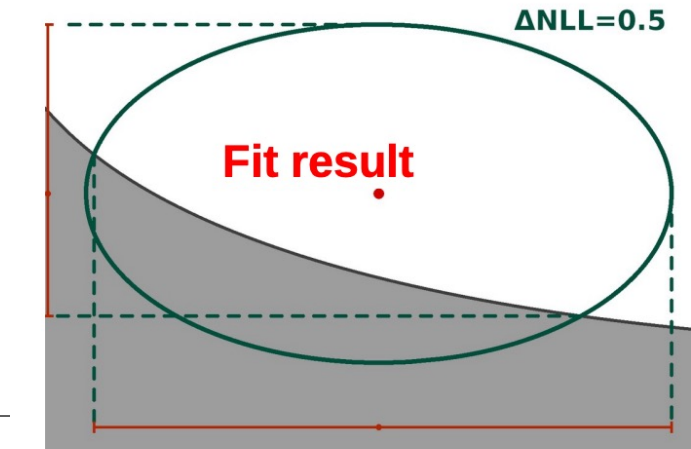
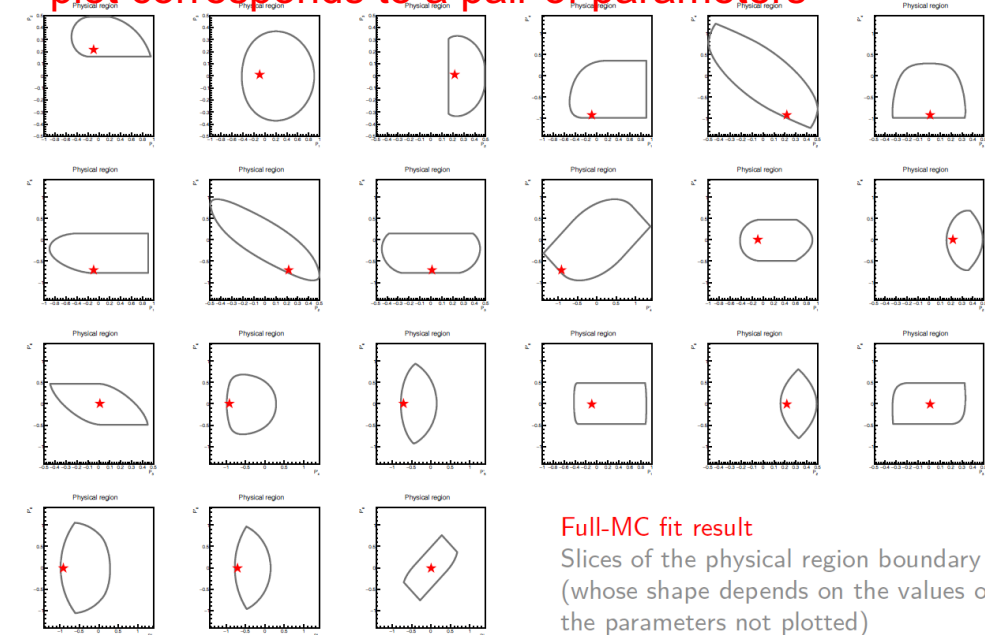
pdf($m, \cos\theta_K, \cos\theta_l, \phi$) = $Y_S [S^C(m) S^a(\cos\theta_K, \cos\theta_l, \phi) \epsilon^C(\cos\theta_K, \cos\theta_l, \phi)$
Angular rate $+ R \cdot S^M(m) S^a(-\cos\theta_K, -\cos\theta_l, -\phi) \epsilon^M(\cos\theta_K, \cos\theta_l, \phi)]$
Signal and bkg mass shapes $+ Y_B B^m(m) B^a(\cos\theta_K, \cos\theta_l, \phi)$
KDE efficiency
Bkg angular shape



物理边界和统计误差

- Physical region: the decay rate is guaranteed to be positive for any values of three angles, a 7-dimensional requirements on P'_i parameters
 - ◆ For full MC sample: fit results are always physical
 - ◆ For data-like statistics MC subsamples: only a fraction of the fit converges to a physical result, a penalized likelihood is used to obtain a physical result from the rest of the samples
- Statistical uncertainty extracted with likelihood profile on each parameter
 - ◆ $\Delta NLL=0.5$ contour of the fit likelihood profile on each parameter
 - ◆ Method accounts for limits of physical region in parameter space

2D slice of the physical region for q^2 bin 2, each plot corresponds to a pair of parameters



效率描述

- **Evaluated from MC for CT and WT separately**

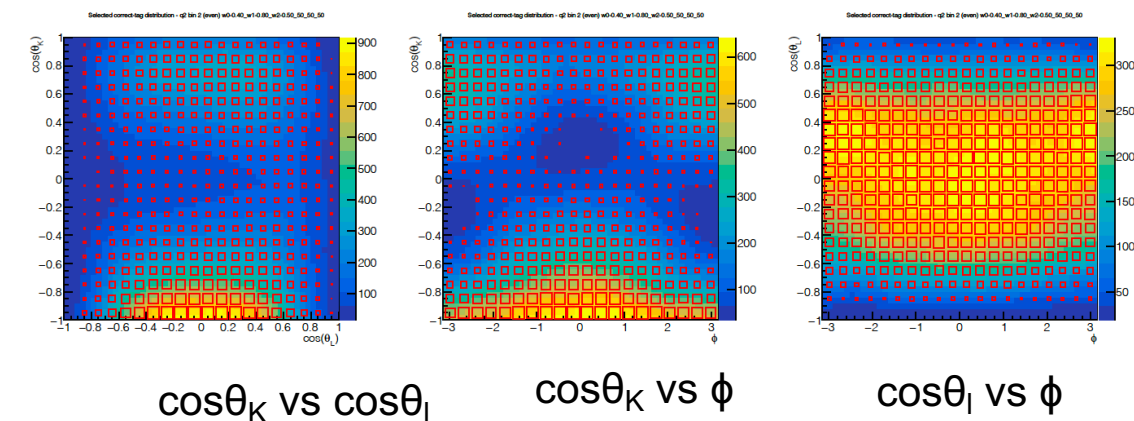
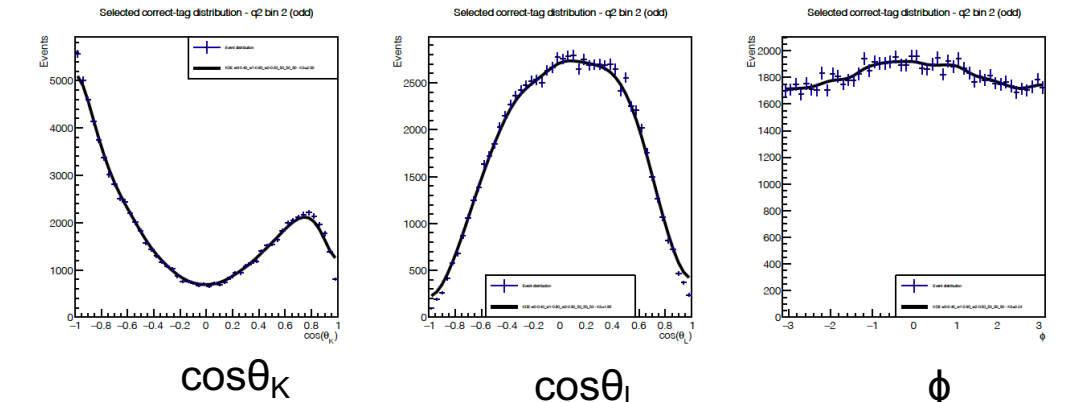
$$\epsilon_c(\cos \theta_K, \cos \theta_l, \phi) = \frac{N_{\text{acc}}(\cos \theta_K, \cos \theta_l, \phi)_{\text{GEN}}}{D_{\text{acc}}(\cos \theta_K, \cos \theta_l, \phi)_{\text{GEN}}} \cdot \frac{N_{\text{sel}}^{\text{corr}}(\cos \theta_K, \cos \theta_l, \phi)_{\text{RECO}}}{D_{\text{sel}}(\cos \theta_K, \cos \theta_l, \phi)_{\text{GEN}}}$$

$$\epsilon_w(\cos \theta_K, \cos \theta_l, \phi) = \frac{N_{\text{acc}}(-\cos \theta_K, -\cos \theta_l, -\phi)_{\text{GEN}}}{D_{\text{acc}}(-\cos \theta_K, -\cos \theta_l, -\phi)_{\text{GEN}}} \cdot \frac{N_{\text{sel}}^{\text{wrong}}(\cos \theta_K, \cos \theta_l, \phi)_{\text{RECO}}}{D_{\text{sel}}(-\cos \theta_K, -\cos \theta_l, -\phi)_{\text{GEN}}}$$

- **Method to describe distributions as sum of multi-variate Gaussians**
- **Applied on numerators and denominators, then ratio is performed on the functions**

q^2 bin 2 2016

1D and 2D projections of KDE function for correct tag





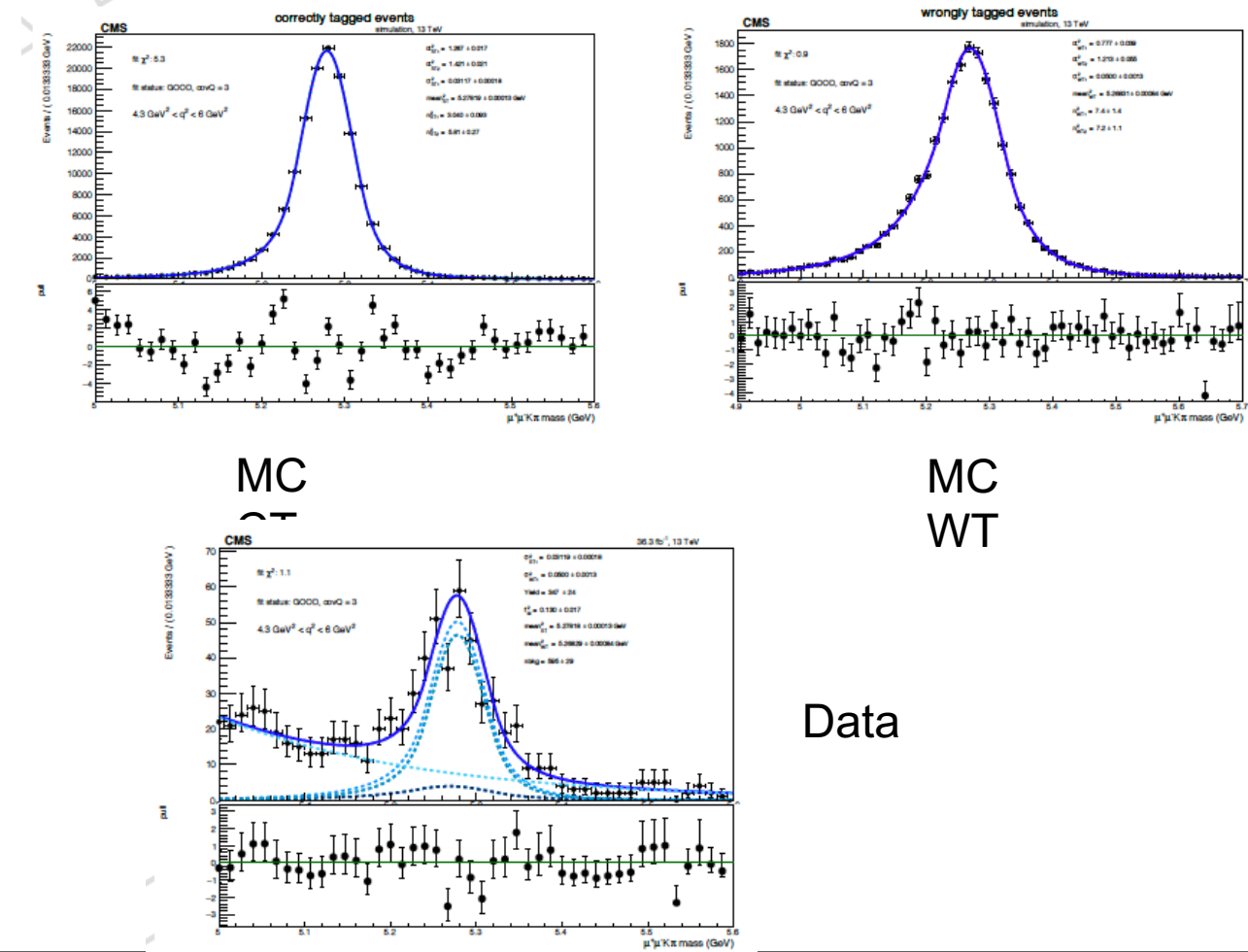
拟合策略总结

	Params	2016	2017	2018
Signal angular pdf	F_L P_1 P_2 P_3 P'_4 P'_5 P'_6 P'_8		$[0, 1]$ $[-1, 1]$ $[-0.5, 0.5]$ $[-0.5, 0.5]$ $[-\sqrt{2}, \sqrt{2}]$ $[-\sqrt{2}, \sqrt{2}]$ $[-\sqrt{2}, \sqrt{2}]$ $[-\sqrt{2}, \sqrt{2}]$	
Signal mass pdf RT	$\sigma_{RT1}, \sigma_{RT2}, \alpha_{RT1},$ $\alpha_{RT2}, n_{RT1}, n_{RT2}, f^{RT}$	constr. to MC	constr. to MC	constr. to MC
	m_{RT}	free	free	free
Signal mass pdf WT	$(m_{WT} - m_{RT}), \sigma_{WT}, \alpha_{WT1}, \alpha_{WT2},$ n_{WT1}, n_{WT2}, f^{WT}	constr. to MC	constr. to MC	constr. to MC
Mistag corr. factor	R	constr. to MC	constr. to MC	constr. to MC
Bkg mass shape	slope	free	free	free
Bkg angular shape	various c_i	fixed from sb	fixed from sb	fixed from sb
Yields	Y_S, Y_B	free	free	free

$K\pi\mu\mu$ 不变质量谱的描述

- Mass model for each signal component (CT and WT) are modeled on MC
 - parametrized by a Double Crystal-ball function or combination of Gaussian and Crystal-ball functions used (according to q^2 bin)

- The data mass distribution is then fit with the model defined on the MC
 - means, widths, mistag fraction have gaussian constraints to values fitted on signal MC
 - The background is parametrized using an exponential function



基于模拟样本的封闭性检验

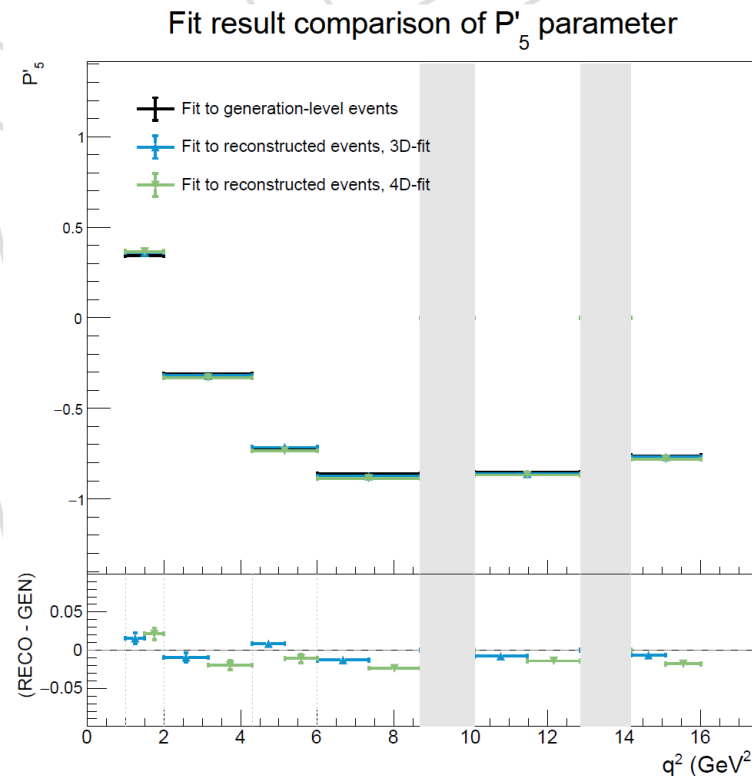
全蒙卡样本

- ◆ 3D Fit to Gen-level MC

- Use pure decay rate as pdf, reference values in the following validation steps

- ◆ Fit to Reco-level MC

- angular decay rate times efficiency, add signal mass shape when perform 4D fit



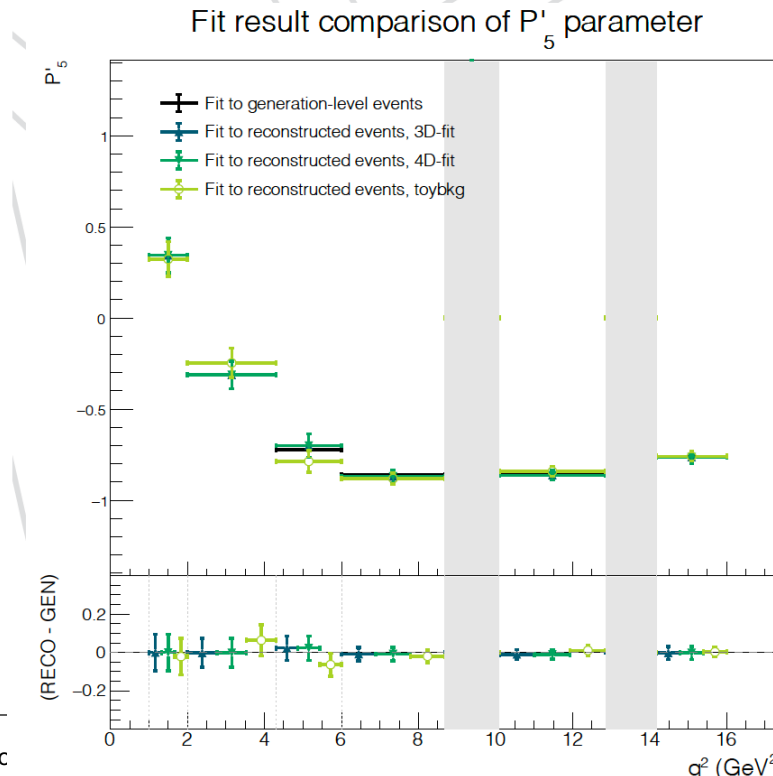
2025/7/12

类数据统计量模拟样本

- ◆ validation on toy samples are performed in 3 steps

- 3D fit to data-like statistics signal only
- 4D fit to data-like statistics signal only
- 4D fit to cocktail toy samples

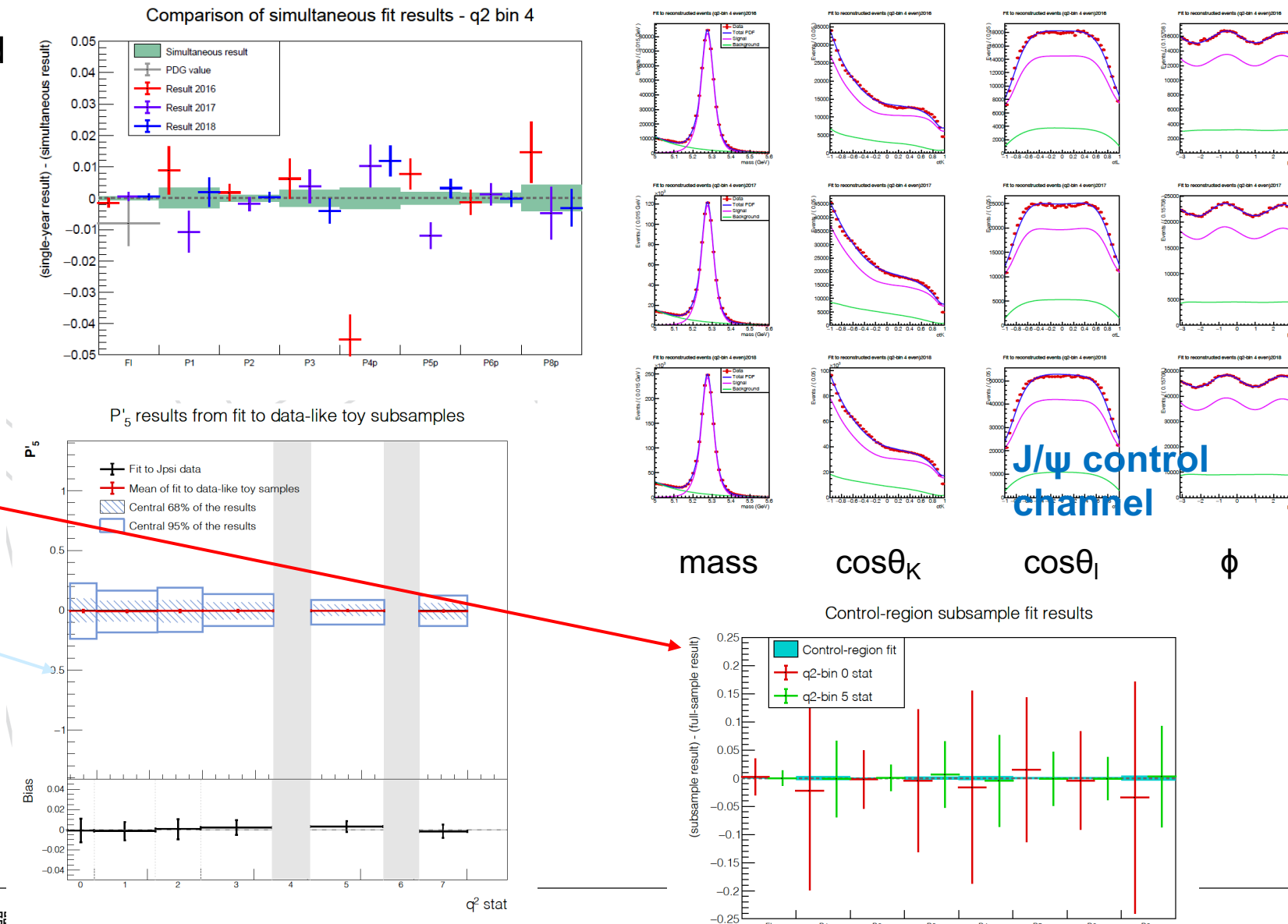
- ◆ Validate the fit procedure with data-like statistics and background



20

封闭性检验—控制道

- Full fit procedure validated on control channels data samples (adding the S-wave component to the pdf)
- Fit validation also perform on data-like samples
 - Subsamples of J/ψ channel dataset
 - Toy samples generated from J/ψ channel fit model
- Validate the fit method in realistic signal q^2 bin



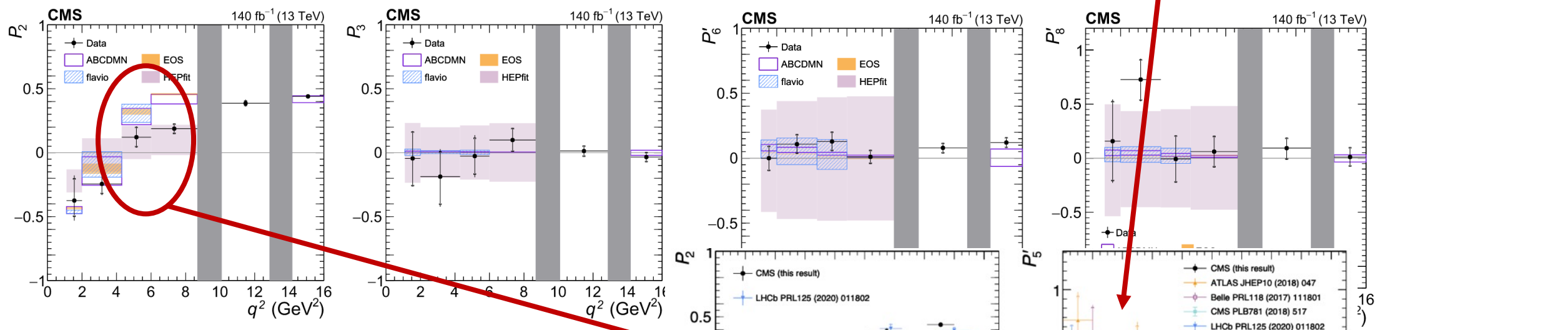
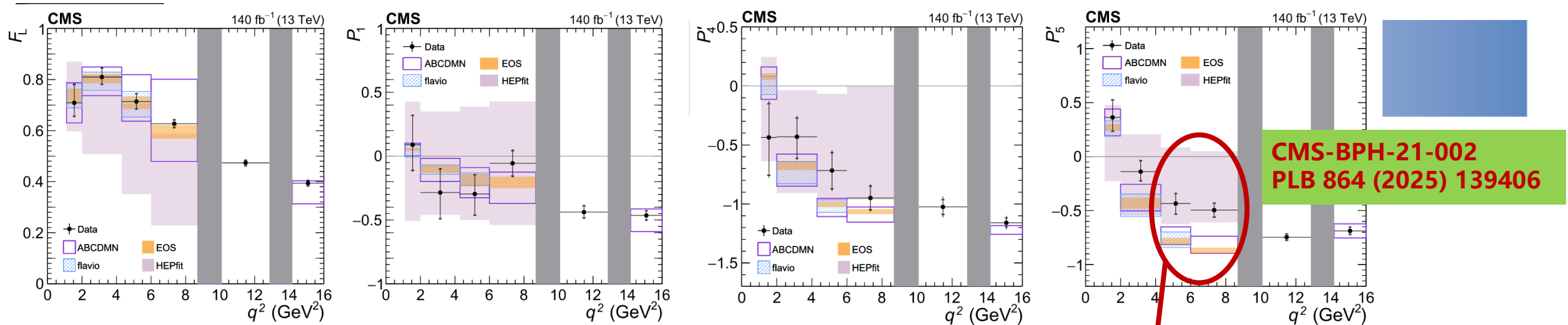


系统误差

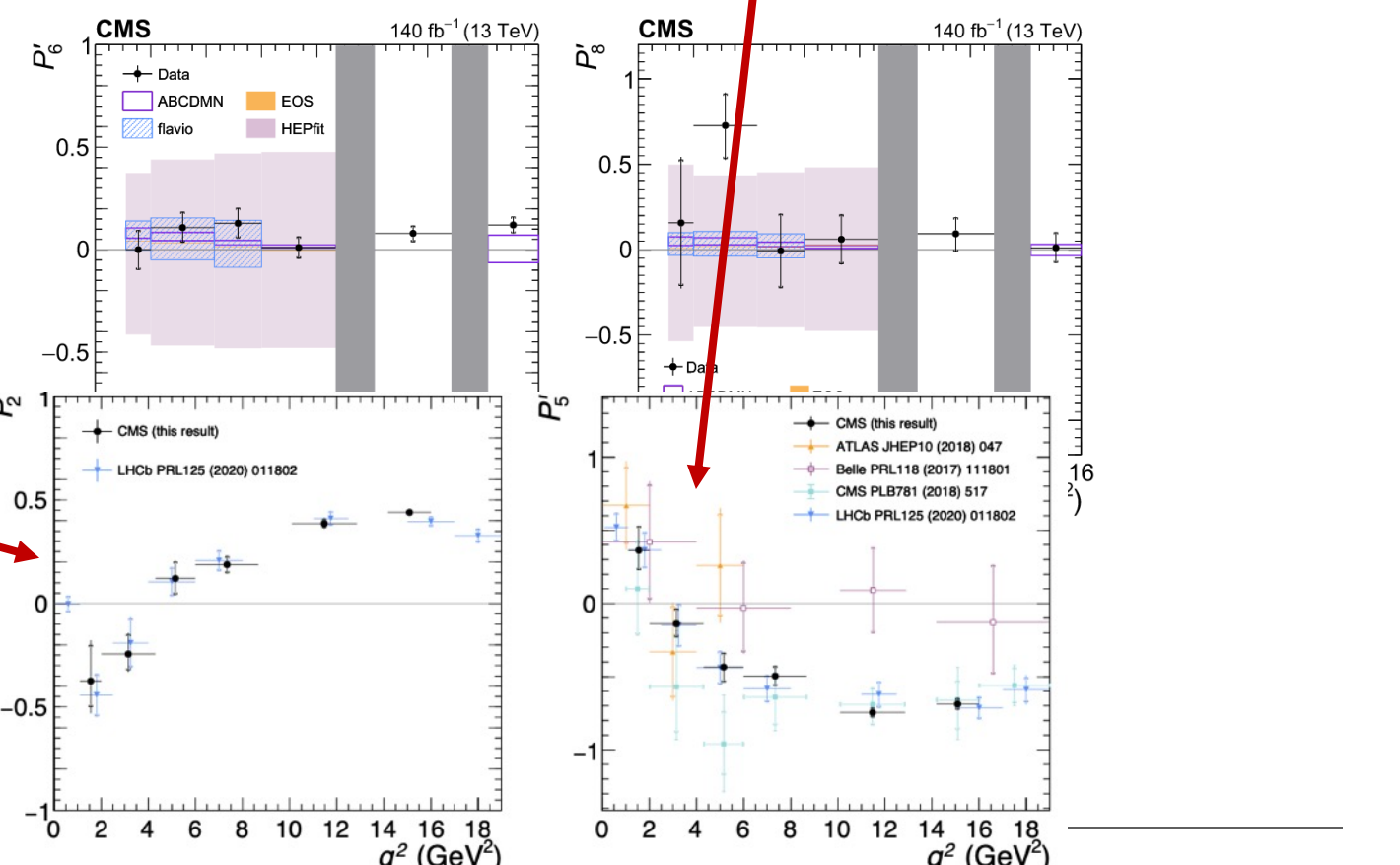
- **MC statistics:** propagation of the statistical fluctuation of the distribution of MC events
- **Sideband statistical uncertainty:** statistical fluctuation on the angular distribution of the data sideband
- **Partially-reconstructed background:** remove a fraction of the low mass sideband from the fit procedure, and use the difference of the results as systematic uncertainty
- **Resonant background:** add a MC-based component to describe the leaking contribution of resonant channels

Source	$F_L (\times 10^{-3})$	$P_1 (\times 10^{-3})$	$P_2 (\times 10^{-3})$	$P_3 (\times 10^{-3})$
Efficiency modeling	1-9	7-44	3-11	0-46
Fit bias	1-2	0-6	2-62	1-12
Mistag fraction	0-2	1-4	1-3	0-14
Signal mass resolution	1-10	1-12	2-11	1-21
Signal mass shape	0-9	1-22	0-10	3-70
Background mass shape	0-5	1-16	1-13	0-8
MC statistics	1-10	5-31	1-64	4-45
Background statistics	2-6	4-20	1-21	2-16
Data/MC differences	8-8	0-23	0-16	0-13
Partially reco bkg	1-1	1-1	0-0	1-1
Resonant bkg	0-1	0-6	0-5	0-2

Source	$P'_4 (\times 10^{-3})$	$P'_5 (\times 10^{-3})$	$P'_6 (\times 10^{-3})$	$P'_8 (\times 10^{-3})$
Efficiency modeling	3-87	2-13	5-16	6-28
Fit bias	9-54	0-8	0-3	0-24
Mistag fraction	1-5	1-10	0-4	0-12
Signal mass resolution	4-23	0-12	0-5	0-16
Signal mass shape	2-16	1-15	0-7	0-91
Background mass shape	6-30	1-13	0-7	1-10
MC statistics	5-47	4-22	4-13	10-59
Background statistics	6-37	4-24	3-9	5-23
Data/MC differences	0-11	0-13	0-3	0-30
Partially reco bkg	25-25	0-0	0-0	2-2
Resonant bkg	0-30	0-11	0-5	0-12



- ✓ among the most precise measurements of the angular observables of this decay
 - ✓ valuable contribution to the understanding of the $b \rightarrow s l^+l^-$



New projection. For each q^2 bin:

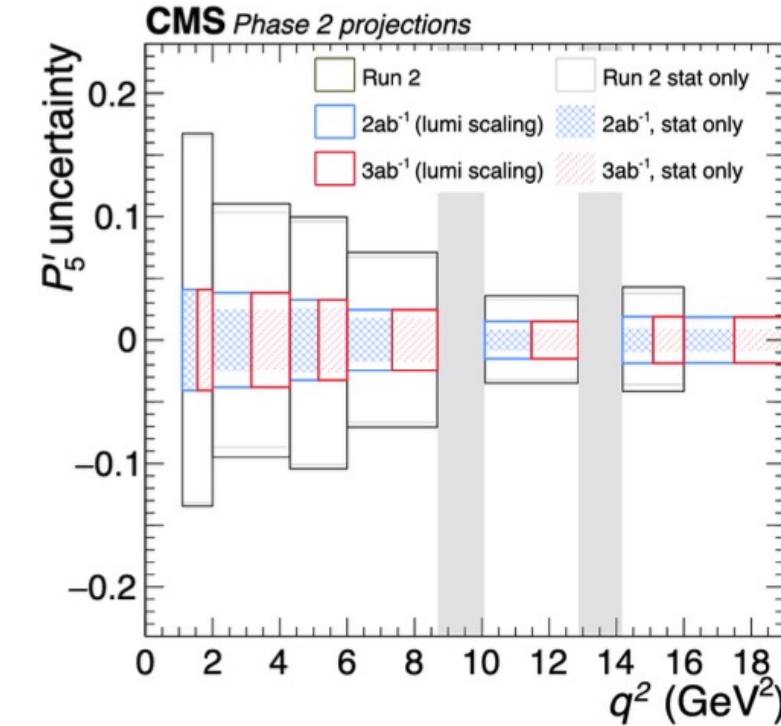
- Yields scaled for $\int L$ and bb-cross section (14/13 TeV) ratio
- Stat. error obtained scaling the Run2 uncertainty by \sqrt{L} ratio
- Syst. error related to $N(B)$ in the sideband scaled by \sqrt{L} ratio
- No syst. related to MC statistics
- For other systematics 2 scenarios: same as Run2 or reduced by a factor 2 wrt Run2

CMS-BPH-25-004
arXiv:2503.24346

Flavour inputs to ESPPU

q^2 bin [GeV 2]	P'_4 (x10 $^{-3}$)			P'_5 (x10 $^{-3}$)			P'_6 (x10 $^{-3}$)			P'_8 (x10 $^{-3}$)		
	σ_{st}	σ_{sy}	σ_{sy}^l									
1.1 – 2	64	47	94	31	5	11	20	8	16	77	48	95
2 – 4.3	36	31	60	20	15	29	15	7	13	39	20	39
4.3 – 6	32	31	62	21	10	19	15	4	7	45	7	13
6 – 8.68	21	25	49	14	9	17	11	7	13	30	18	35
10.09 – 12.86	14	28	57	7	6	12	8	5	10	21	11	22
14.18 – 16	8	20	40	8	8	16	8	4	9	18	8	17
16 – 19	8	20	40	7	8	16	8	4	9	17	8	17

Statistical error still dominant

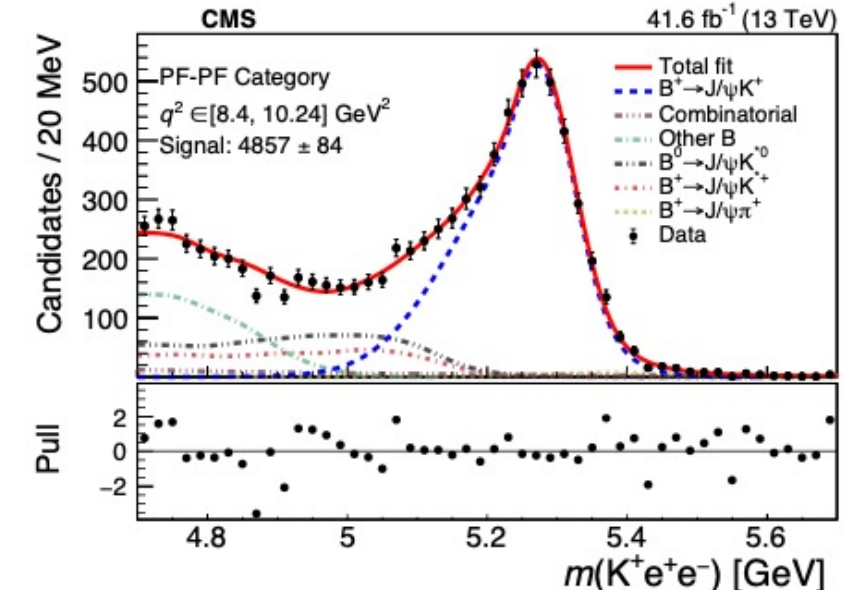
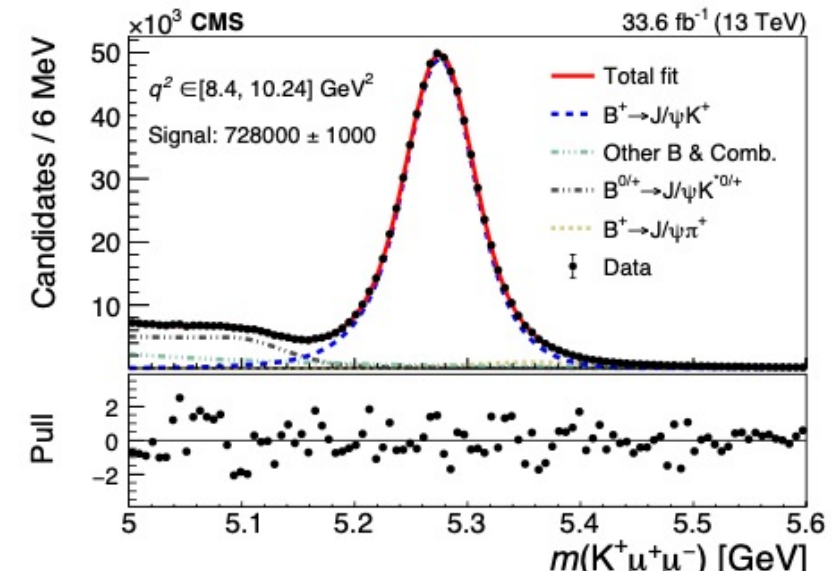


Measurements of $B^+ \rightarrow K^+ \bar{K} \bar{K}$ with B parking data

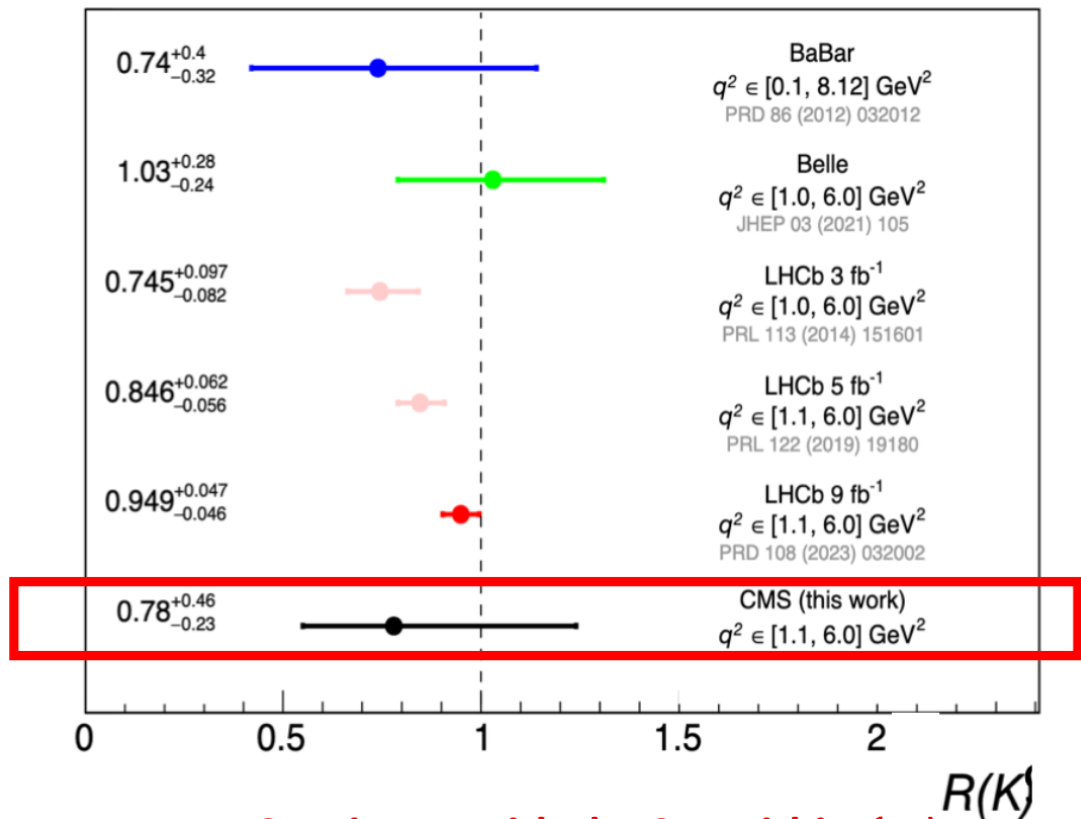
$$\mathcal{R}(K) = \frac{\mathcal{B}(B \rightarrow \mu\mu K)}{\mathcal{B}(B \rightarrow J/\psi(\rightarrow \mu\mu)K)} / \frac{\mathcal{B}(B \rightarrow eeK)}{\mathcal{B}(B \rightarrow (B \rightarrow J/\psi(\rightarrow ee)K))}$$

- Theoretical precision: 1.00 ± 0.01
- New data-acquisition technique: 2018 B-Parking
- Fit to $K\bar{K}\bar{K}$ invariant mass in 3 q^2 regions,
 - ◆ SR: (1.1, 6.0) GeV, J/ψ CR: (8.41, 10.24) GeV $\psi(2S)$ CR: (12.6, 14.4) GeV
- Dedicated low-pT ID for electrons
- Main Backgrounds suppressed mostly through ID BDTs:
 - ◆ Partially reconstructed $B \rightarrow K^*(892)\bar{K}$
 - ◆ J/ψ leakage and any other B decays
 - ◆ Combinatorial
- Ratio extracted from profile likelihood

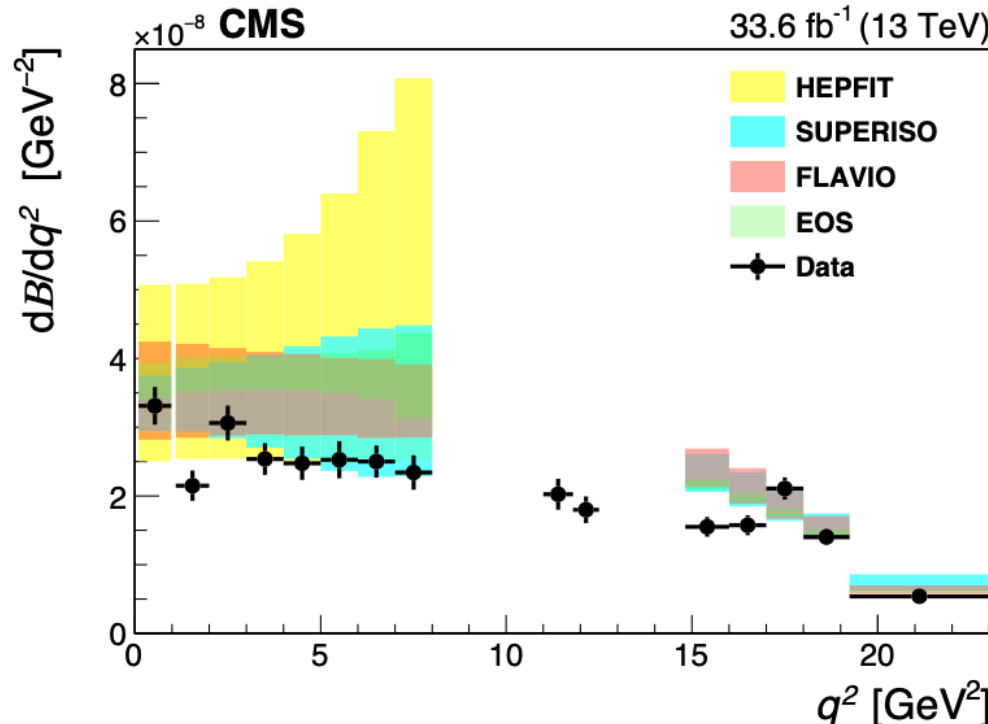
$$R(K) = 0.78^{+0.46}_{-0.23} \text{ (stat)}^{+0.09}_{-0.05} \text{ (syst)} = 0.78^{+0.47}_{-0.23},$$



Source	Impact on the $R(K)$ ratio [%]	
	PF-PF	PF-LP
Signal and background description	5	5
J/ ψ event leakage to the low- q^2 bin	4	9
BDT efficiency stability	2	5
BDT cross validation	2	3
Trigger efficiency	1	4
BDT data/simulation difference	1	2
J/ ψ meson radiative tail description	1	1
Total systematic uncertainty	7	13
Statistical and total uncertainty	40	200



Consistent with the SM within 1σ !



$$\mathcal{B}(B^\pm \rightarrow K^\pm \mu^+ \mu^-) = (12.42 \pm 0.68) \times 10^{-8}$$

consistent with and has a comparable precision to the present world average

CMS-BPH-22-005
Rep. Prog. Phys. 87 (2024) 077802

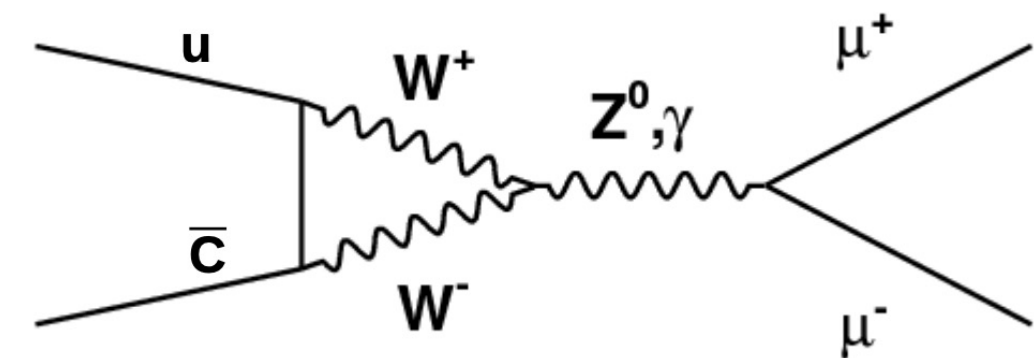
Search for $D^0 \rightarrow \mu\mu$ decay

- **Heavily suppressed in the SM (loop diagram + helicity)**

- ◆ BR prediction $\sim 10^{-13}$
- ◆ High sensitivity to new-physics phenomena
- ◆ Previous best limit at: $\text{BR}(D^0 \rightarrow \mu\mu) < 3.5 \times 10^{-9}$ (95% CL) by LHCb

- **This analysis uses 2022+2023 CMS data with new low-momentum dimuon trigger**

- ◆ a newly developed inclusive dimuon trigger, expanding the scope of the CMS flavor physics program.





Key points of the search

■ Analysis Strategy

- ◆ uses D⁰ from cascade decays: $D^{*+} \rightarrow D^0 \pi^+$
- ◆ Exploits mass difference $\Delta m = m(D^{*+}) - m(D^0)$ to strongly suppress combinatorial
- ◆ D^{*+} produced promptly or from B-hadron decays
- ◆ Final state: opposite charged muons + track

■ $D^0 \rightarrow \pi^+ \pi^-$ used as normalization channel:

$$\mathcal{B}(D^0 \rightarrow \mu^+ \mu^-) = \mathcal{B}(D^0 \rightarrow \pi^+ \pi^-) \frac{N_{D^0 \rightarrow \mu\mu}}{N_{D^0 \rightarrow \pi\pi}} \frac{\varepsilon_{D^0 \rightarrow \pi\pi}}{\varepsilon_{D^0 \rightarrow \mu\mu}}$$

■ Source of backgrounds

- ◆ Combinatorial: suppressed via gradient BDT, exploiting topological features
- ◆ Peaking backgrounds for signal:
 - $D^{*+} \rightarrow D^0 (\pi\pi)\pi \rightarrow \mu\mu + X$
 - $D^{*+} \rightarrow D^0 (\pi\mu\nu)\pi$
- ◆ Peaking background for normalization channel:
 - $D^{*+} \rightarrow D^0 (K\pi)\pi$



Search results

2D UML fits:

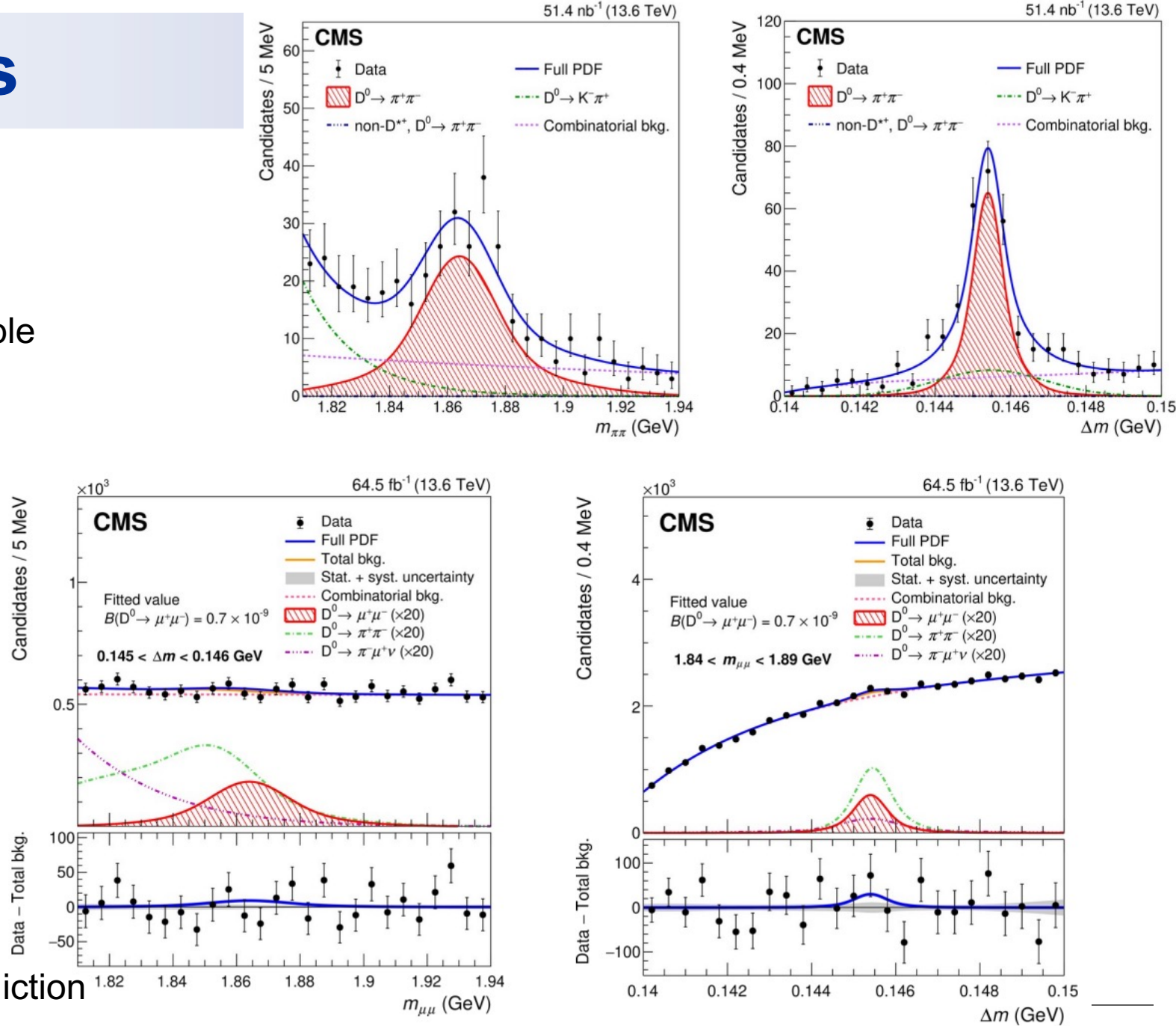
- to $[m(\pi\pi), \Delta m]$ in normalization sample
- to $[m(\mu\mu), \Delta m]$ in signal sample

$B(D^0 \rightarrow \mu^+\mu^-) < 2.1(2.4) \times 10^{-9}$ at
90(95)% CL, upper limit improved by
 $\sim 40\%$

the most stringent upper limit set
on any flavor changing neutral
current decay in the charm sector

CMS-BPH-23-008
Arxiv:2506.06152

Still 4 order of magnitude above SM prediction



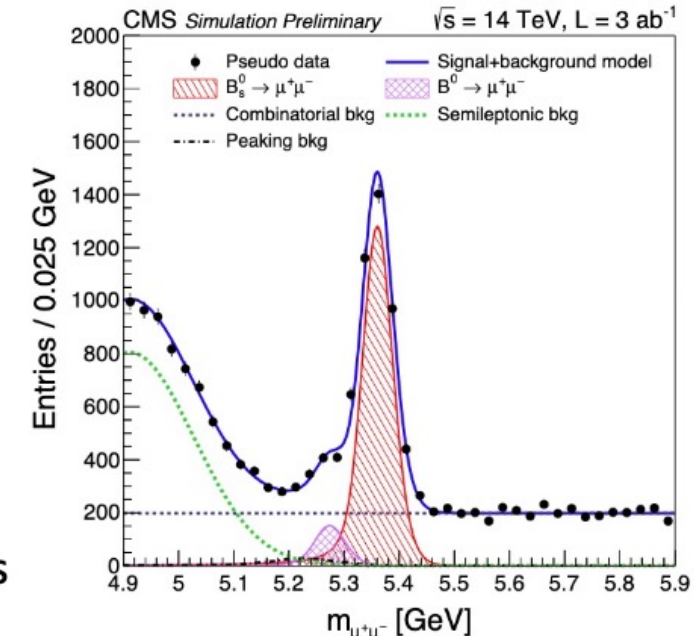
CMS B_s and $B^0 \rightarrow \mu\mu$: HL-LHC projections

CMS-BPH-25-004
arXiv:2503.24346

Flavour inputs to ESPPU

New projection:

- Yields scaled for $\int L$ and cross section (14/13 TeV) ratio
- Improved mass resolution included as scaling factor
- Same integrated S/B ratio as in the current analysis
- Stat. uncertainty from fits to pseudo-data
 - with s-plots weights for the lifetime
- Same syst. uncertainty as in Run2. Exceptions:
 - 1.5% instead 2.3% in tracking efficiency
 - 2.4% trigger efficiency uncertainty, uniform across categories
 - **Total: 3.5% from f_s/f_u ratio; 4.3% for all other sources**
 - x2 improvement for lifetime fit bias and the mismodeling of the decay time distribution



Systematics becomes relevant for B_s ; Clear observation of $B^0 \rightarrow \mu\mu$ possible

\mathcal{L}	$N(B_s^0)$	$N(B^0)$	$\delta\mathcal{B}(B_s^0 \rightarrow \mu\mu)$			$\delta\mathcal{B}(B^0 \rightarrow \mu\mu)$	$B^0 \rightarrow \mu\mu$	$\delta\tau(B_s^0 \rightarrow \mu\mu)[\text{ps}]$			
			stat.	syst.	f_s/f_u	total		stat.	syst.	total	
2 ab^{-1}	2539	302	5.0%	3.5%	6.1%		14%	7.4–9.7 σ	0.044	0.026	0.051
3 ab^{-1}	3808	452	4.8%	3.5%	5.9%		12%	9.1–11.5 σ	0.036	0.026	0.044

* Medians of 5k toys

in a $\pm 1\sigma$ range



Summary

- CMS is probing SM with heavy hadrons extensively
- Many new results from heavy hadron studies
 - ◆ B and D FCNC processes
 - Run2: Full angular analysis of $B^0 \rightarrow K^{*0} \mu\mu$, PLB 864 (2025) 139406
 - BF measurement and LFU test of $B^+ \rightarrow K^+ \ell \ell$: Rep. Prog. Phys. 87 (2024) 077802
 - $D^0 \rightarrow \mu\mu$: arxiv:2506.06152
 - ◆ Conventional and exotic hadron spectroscopy
 - ◆ Heavy hadron production and polarization measurements
 - ◆ CKM triangle and CP violation
 - ◆
- More Flexible trigger and data-taking schemes implemented in Run3, more sensitive results expected
 - ◆ HL-LHC coming in ~5 years, projections updated

More:
[CMS Public Results](#)



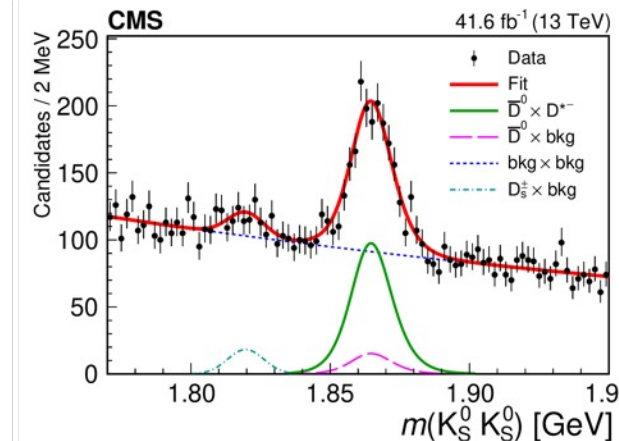
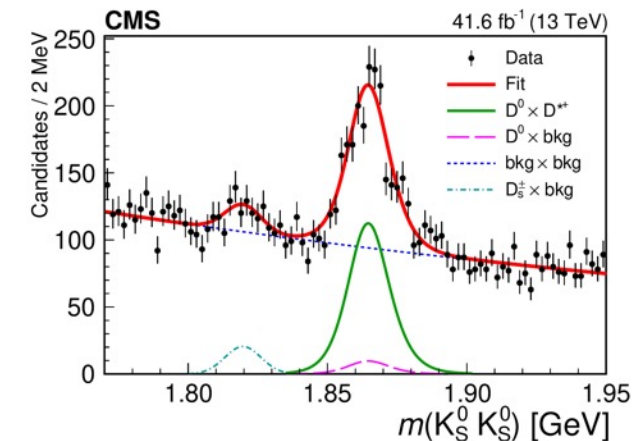
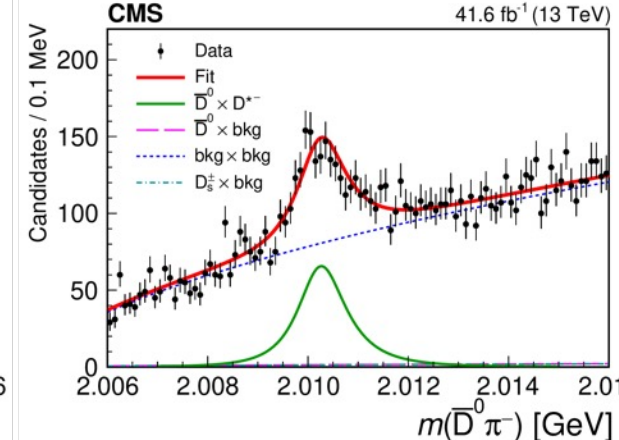
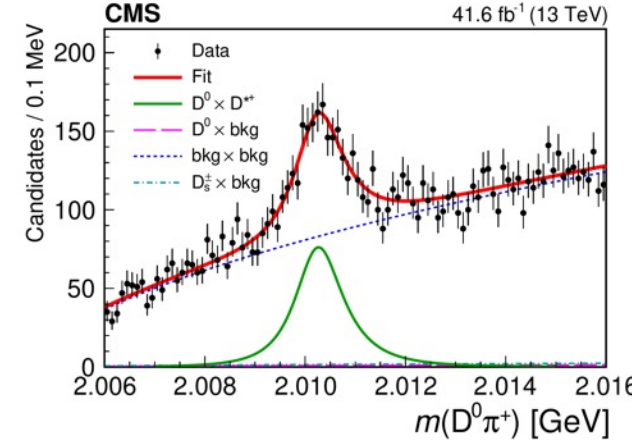
Back up



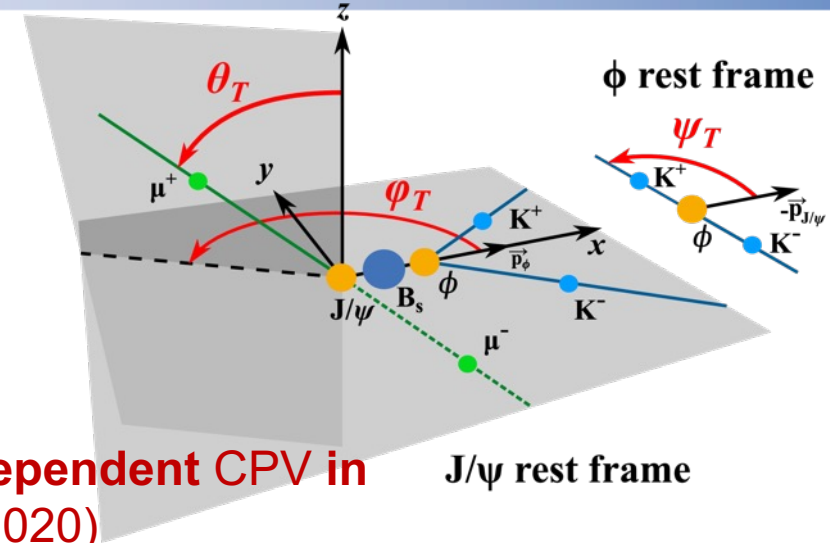
Studies of CP violation in charm and beauty

$$D^0 \rightarrow K_S^0 K_S^0$$

CMS-BPH-23-005
EPJC 84 (2024) 1264



$$A_{CP}(K_S^0 K_S^0) = (6.2 \pm 3.0 \pm 0.2 \pm 0.8)\%$$



3.2 σ time-dependent CPV in

$$B_s^0 \rightarrow J/\psi \phi(1020)$$

